

# ***Ab initio* statistical thermodynamical models for the computation of third-law entropies**

Allan L. L. East<sup>a)</sup>

Research School of Chemistry, Australian National University, Canberra, ACT 0200, Australia and Steacie Institute for Molecular Sciences, National Research Council, Ottawa, Ontario K1A 0R6, Canada

Leo Radom

Research School of Chemistry, Australian National University, Canberra, ACT 0200, Australia

(Received 12 September 1996; accepted 16 January 1997)

Third-law gas-phase statistical entropies are computed for a variety of closed-shell singlet state species using standard formulae based upon canonical partition functions. Molecular parameters are determined *ab initio*, and sensitivity analyses are performed to determine expected accuracies. Several choices for the canonical partition function are examined for internal rotations. Three general utility procedures for calculating the entropies are developed and designated E1, E2, and E3 in order of increased accuracy. The E1 procedure adheres to the harmonic oscillator approximation for all vibrational degrees of freedom other than for very low barrier internal rotations, these being treated as free rotations, and yields entropies to an accuracy of better than  $1 \text{ J mol}^{-1} \text{ K}^{-1}$  for molecules with no internal rotations. For molecules with internal rotations, errors of up to  $1.8 \text{ J mol}^{-1} \text{ K}^{-1}$  per internal rotation are observed. Our E2 procedure, which treats each individual internal rotation explicitly with a simple cosine potential, yields total entropies to an accuracy of better than  $1 \text{ J mol}^{-1} \text{ K}^{-1}$  for species with zero or one internal rotation, and better than  $2 \text{ J mol}^{-1} \text{ K}^{-1}$  for species with two internal rotation modes. Rotor-rotor coupling is found to contribute on the order of  $1 \text{ J mol}^{-1} \text{ K}^{-1}$  for a third-law entropy. Our E3 procedure takes this into account and, with the aid of new *ab initio* two-dimensional torsional potential energy surfaces of state-of-the-art accuracy, improves the accuracy of the predicted entropy for species with two internal rotation modes to approximately  $1 \text{ J mol}^{-1} \text{ K}^{-1}$ . © 1997 American Institute of Physics.

[S0021-9606(97)50616-7]

## **I. INTRODUCTION**

Absolute third-law entropies for gases, as calculated from spectroscopic data, have found common use as an accurate means of computing gas-phase reaction entropies. There are several sources available which list standard entropies for a multitude of neutral compounds computed in this way.<sup>1-3</sup> However, for many molecules, and particularly ions, spectroscopic data are not available, and hence first-principles thermodynamic results cannot be obtained in this manner.

An alternative source for reaction entropies comes directly from measurements of the temperature dependence of equilibrium constants. This has been particularly important in the area of gas-phase ion chemistry. For example, recent extensive experimental effort (see for example, Refs. 4-9) has been directed towards obtaining scales of gas-phase proton affinities, i.e., enthalpy changes for reactions



and entropies play an important role in the analysis. The two principal experimental procedures for obtaining the quantitative data required for setting up proton affinity scales both involve measuring the equilibrium constant ( $K$ ) for proton-transfer reactions of the type



The single-temperature experiments must *assume* a value for  $\Delta S$  in order to determine  $\Delta H$ , while the variable-temperature experiments *produce* a value for  $\Delta S$  from the van't Hoff plot of  $\ln K$  versus inverse temperature.

Theory has also been able to make a valuable contribution to the study of the thermodynamics of proton-transfer reactions. For example, extensive recent studies<sup>10-13</sup> have demonstrated excellent agreement between experimental proton affinities and values calculated at the G2 level of theory<sup>14</sup> and some of its simplified variants. There remain some discrepancies among experimental results for enthalpies and entropies of proton-transfer reactions, however, suggesting that a parallel *ab initio* investigation of absolute third-law entropies of gas-phase molecules and their protonated cations would be quite useful.

The present study examines *ab initio* procedures and statistical thermodynamic models that might be used in general utility procedures for the prediction of molecular entropies. At the one extreme, we aim to develop a model (E1) that produces entropies of reasonable accuracy at minimal cost and which therefore should be capable of widespread application. At the other extreme, we aim to develop a model (E3) that produces entropies of high accuracy at reasonable cost, that would be suitable for more demanding situations. In a companion study, we examine the application of these models to proton-transfer reactions.

<sup>a)</sup>Present address: Steacie Institute for Molecular Sciences, National Research Council, Ottawa, Ontario K1A 0R6, Canada.

The theoretical methods used in the present work are presented in Sec. II. In Sec. III, sensitivity analyses are performed, and in Sec. IV the results of various statistical thermodynamic procedures are presented. In Sec. V, the three general-utility procedures (E1, E2, and E3) selected for complete first-principles computation of third-law entropies are described, and general conclusions are presented in Sec. VI.

## II. THEORETICAL METHODS

Standard *ab initio* molecular orbital calculations<sup>15</sup> were performed at a number of levels of theory, using various versions of the GAUSSIAN<sup>16,17</sup> and MOLPRO<sup>18</sup> codes.

In the section of this work dealing with explorations of levels of *ab initio* theory, a variety of one-electron atomic-orbital basis sets and levels of electron correlation were investigated. Of the eleven Gaussian basis sets which were tested, eight sets are due to Pople and co-workers<sup>19–22</sup> [ranging from 6-31G(*d*) to 6-311+G(3*df*,2*p*)] and three sets are due to Dunning and co-workers<sup>23,24</sup> (cc-pVDZ, aug-cc-pVDZ, and cc-pVTZ). The *d* and *f* shells in all basis sets contain five and seven functions, respectively (i.e., no super-numerary *s* or *p* functions are present), except for *d* shells appended to the 6-31G sets, in which case Cartesian 6*d* sets are standard.

Beyond the molecular orbital approximation of Hartree–Fock (HF) theory, the effect of electron correlation on internal rotation barriers was investigated using Møller–Plesset perturbation theory (MP2, MP3, MP4),<sup>25–28</sup> coupled-cluster<sup>29,30</sup> and quadratic configuration interaction<sup>31</sup> theories including all single and double excitations from the reference configuration (CCSD and QCISD), and the extension of these latter two to incorporate effects of triple excitations via perturbative corrections (CCSD(T), CCSD[T], QCISD(T), and QCISD[T]).<sup>32,33</sup> Core orbitals were frozen in all correlated computations, with all valence and virtual orbitals remaining active.

Analytic gradient techniques<sup>34–36</sup> for the RHF<sup>37,38</sup> and RMP2<sup>39–42</sup> methods were used to perform complete and constrained geometry optimizations of minima and internal rotation maxima, to  $10^{-5}$  Å and  $10^{-3}$  degrees in all but exceptional cases, with the GAUSSIAN program packages. For some transition structure optimizations, the eigenvector-following optimization method of Baker<sup>43</sup> was found to be a significant aid. Analytic HF second derivatives<sup>39,44</sup> for frequency calculations were also performed with GAUSSIAN, while energies were determined using both the GAUSSIAN and the MOLPRO codes.

For the principal body of calculations, geometric structures of the molecules and cations were optimized at the MP2/6-31G(*d*) level of theory (with frozen core-orbitals, unlike G2 theory<sup>14</sup>), while the HF/6-31G(*d*) level of theory was used to obtain harmonic vibrational frequencies at the HF potential surface minima. Energetics for internal rotation modes were obtained from MP2/6-311+G(2*df*,*p*) energies computed using the MP2/6-31G(*d*) geometries.

Standard statistical thermodynamic formulae are employed for the calculation of absolute third-law entropies.

The rigid-rotor-harmonic-oscillator (RRHO) approximation is assumed for all rotation and vibration modes, except for internal rotation modes for which various models were employed. The harmonic oscillator produces poor and fundamentally incorrect results for the entropy of an internal rotation mode when the barrier to rotation becomes vanishingly small (extrapolating to infinite entropy when the barrier drops to zero). Internal rotations are therefore treated not only with the harmonic oscillator approximation, but also with other models using the excellent machinery provided 50 years ago by Pitzer and co-workers,<sup>45–47</sup> as discussed in more detail below. Since all species in this work have straightforward closed-shell singlet electronic structures, electronic contributions to the entropy were neglected. Nuclear spin and isotopic effects are generally neglected as well, with the most abundant isotopes, e.g., <sup>12</sup>C<sup>16</sup>O, being used unless otherwise discussed.

## III. SENSITIVITY ANALYSES

Exploratory analyses were first carried out to determine (i) cost-effective levels of *ab initio* theory to use for the determination of molecular parameters, and (ii) the kind of accuracy one can expect from them. Fortunately, only moderate levels of theory are needed to reduce the errors in entropy down to those of the independent (normal) mode approximation of standard statistical thermodynamics. For systems with strongly coupled low frequency modes, where the normal mode approximation begins to break down for the description of the excited energy levels which are accessed at moderate temperatures, the independent mode approximation itself can present errors of 1 J mol<sup>-1</sup> K<sup>-1</sup> or more in absolute entropy. We thus set 1 J mol<sup>-1</sup> K<sup>-1</sup> accuracy as an ultimate target for our most accurate entropy model (E3), anticipating that for many purposes this should be more than sufficient.

### A. Levels of *ab initio* theory

Let us consider the individual components of the third-law entropy of a mole of identical molecules. Electronic entropy ( $S_{\text{elec}}$ ) is most commonly represented as a contribution of  $R \ln \Omega$ , where  $\Omega$  is the electronic degeneracy of the ground state. In this work, we shall only examine closed-shell-singlet species and hence we can ignore ( $S_{\text{elec}}$ ). The translational entropy ( $S_{\text{trans}}$ ) for ideal gases at a specific temperature and pressure depends only on the molecular mass, and hence is unaffected by choice of *ab initio* method. The entropy due to external molecular rotation ( $S_{\text{rot}}$ ) under the rigid rotor (RR) approximation depends on the principal moments of inertia of the molecule; these are derived from the geometrical parameters which are dependent on the level of *ab initio* theory used in geometry optimization. The entropy due to molecular vibration ( $S_{\text{vib}}$ ) under the harmonic oscillator (HO) approximation depends on the harmonic vibrational frequencies, which can also be determined *ab initio*, but are again dependent on the level of theory employed.

Three levels of theory were tested for the calculation of rotational and vibrational entropies for methanol and water,

TABLE I. Effect of level of theory on calculated vibration and rotation entropies ( $\text{J mol}^{-1} \text{K}^{-1}$ ) at 298.15 K.<sup>a,b</sup>

	HF/6-31G( <i>d</i> )	MP2/6-31G( <i>d</i> )	MP2/6-311G( <i>d,p</i> )	Expt.
CH <sub>3</sub> OH:				
$S^{\text{rot}}$	79.137	79.507	79.413	79.454 <sup>c</sup>
$S^{\text{vib}2}$	0.305	0.320	0.309	0.307 <sup>d</sup>
$S^{\text{vib}1}$	0.333	0.358	0.340	0.343 <sup>d</sup>
H <sub>2</sub> O:				
$S^{\text{rot}}$	43.413	44.022	43.784	43.706 <sup>c</sup>
$S^{\text{vib}2}$	10 <sup>-6</sup>	10 <sup>-6</sup>	10 <sup>-6</sup>	10 <sup>-6</sup> <sup>d</sup>
$S^{\text{vib}1}$	0.028	0.027	0.035	0.033 <sup>d</sup>

<sup>a</sup> $S^{\text{vib}1}$  and  $S^{\text{vib}2}$  indicate individual contributions from the vibrations of lowest frequency and second-lowest frequency. The internal rotation of methanol is not considered a vibrational mode in this context.

<sup>b</sup>Harmonic vibrational frequencies were scaled (Ref. 52) by 0.8929 for HF/6-31G(*d*), 0.9434 for MP2/6-31G(*d*), and 0.9496 for MP2/6-311G(*d,p*).

<sup>c</sup>Using molecular geometry of Harmony *et al.* (Ref. 48).

<sup>d</sup>Using vibrational frequencies from Shimanouchi (Ref. 49).

<sup>e</sup>Using molecular geometry of Hoy *et al.* (Ref. 50).

and the results are compared in Table I with those obtained using experimental molecular parameters.<sup>48–50</sup> For rotational entropy, each estimate is within  $0.33 \text{ J mol}^{-1} \text{K}^{-1}$  of the values obtained using experimental geometries. As Hartree–Fock bond lengths are generally too short, the entropy estimates derived from them will generally be too low. With regards to the MP2 results, the larger 6-311G(*d,p*) basis set improves the rotational entropy estimate for water by  $0.24 \text{ J mol}^{-1} \text{K}^{-1}$  relative to the MP2/6-31G(*d*) result, but for methanol the results are equally good. The smaller basis set can be applied to a larger range of molecules due to lower computational requirements, and hence the MP2/6-31G(*d*) level of theory was chosen as the standard for the general optimization of structures for rotational entropy.

The vibrations which contribute most to the absolute entropy are those of lowest frequency, and only the two largest contributions appear in Table I. The systematic overestimation of vibrational frequencies by the HF and MP2 levels of theory produce systematic underestimation of vibrational entropies. Not only can these accumulate for molecules with several low-frequency vibrations, but a 5% overestimation of a low frequency (which is the typical error observed with MP2 theory) causes a 15–30% underestimation of its entropy (based on our results for water and methanol). In addition, thermodynamic results using the harmonic oscillator approximation are improved by using the true vibrational fundamental  $\nu$  rather than the harmonic frequency  $\omega$ . Hence we employ the common practice of empirically scaling the *ab initio* harmonic frequencies, and report results so obtained.<sup>51,52</sup> The two largest vibrational entropy contributions are insignificant for water, while for methanol they each contribute  $0.3 \text{ J mol}^{-1} \text{K}^{-1}$ , and are predicted to within  $0.02 \text{ J mol}^{-1} \text{K}^{-1}$  for each level of theory after scaling. The HF/6–31G(*d*) method with its well-established scaling factor (0.8929)<sup>51</sup> was chosen for vibrational entropies. We note that these levels of theory, which represent a compromise between accuracy and efficiency, are the same as those used in G2 calculations,<sup>14</sup> with the minor difference, as noted ear-

TABLE II. Sensitivity of hindered rotor entropy ( $\text{J mol}^{-1} \text{K}^{-1}$ ) to adjustments in barrier height and moment of inertia at 298.15 K.<sup>a</sup>

$V_0$ ( $\text{kJ mol}^{-1}$ )	$I$ ( $\text{amu} \text{Å}^2$ )			
	0.65	0.70	2.80	3.00
4	7.58	7.87	13.40	13.69
5	7.19	7.47	12.88	13.17
10	5.00	5.23	10.08	10.36
11	4.62	4.84	9.59	9.86

<sup>a</sup>Entries are derived from the tables of Pitzer *et al.* (Refs. 45 and 53) with symmetry number  $\sigma=3$ .

lier, being that in G2 theory the geometrical structures are optimized without freezing the core electrons in the MP2 calculations. This distinction is unlikely to lead to any significant differences in calculated entropies.

For hindered internal rotations, the potential energy is better described by the cosine potential

$$V(\alpha) = (V_0/2)(1 - \cos n\alpha), \quad (3)$$

rather than the harmonic potential. In this expression,  $\alpha$  is the torsional angle,  $n$  the periodicity of the rotation, and  $V_0$  the barrier height. In this case, the contribution to absolute entropy can be found from the tables of Pitzer and co-workers.<sup>45,53</sup> These tables provide values of the entropy as a function of  $V_0/RT$  and  $1/Q_f$ , where  $R$  is the gas constant ( $8.31451 \text{ J mol}^{-1} \text{K}^{-1}$ ),  $T$  is temperature, and  $Q_f$  is the partition function of the free (unhindered) internal rotor, which itself is a function of temperature, the rotor symmetry number  $\sigma$ , and the internal rotor moment of inertia  $I$ . In order to gauge the effects of errors in  $V_0$  and  $I$  on this entropy, the Pitzer tables were used to produce Table II. The values of most interest in this work are values for methyl groups rotating against massive groups (the right side of Table II) and the internal rotation in methanol (the upper left of Table II). The results indicate that a change in  $V_0$  of  $1 \text{ kJ mol}^{-1}$  leads to a change in entropy of  $0.4\text{--}0.5 \text{ J mol}^{-1} \text{K}^{-1}$ , while a change in  $I$  of  $0.05 \text{ amu} \text{Å}^2$  leads to a change in entropy of  $0.1\text{--}0.3 \text{ J mol}^{-1} \text{K}^{-1}$ . Hence, in order to restrict the error in the internal rotation contribution to the entropy to a target of  $0.3 \text{ J mol}^{-1} \text{K}^{-1}$  at 298 K,  $V_0$  and  $I$  need to be accurate to approximately  $0.8 \text{ kJ mol}^{-1}$  and  $0.05 \text{ amu} \text{Å}^2$ , respectively. At 600 K the requirement on  $V_0$  is slightly more relaxed, with  $1.0 \text{ kJ mol}^{-1}$  accuracy in  $V_0$  being sufficient for the same  $0.3 \text{ J mol}^{-1} \text{K}^{-1}$  target accuracy in hindered rotor entropy.

Barrier heights can be straightforwardly obtained using *ab initio* methods. Results are presented in Table III and Table IV for the barrier height for internal rotation of methanol. These test runs were performed to determine a level of theory suitable for the computation of barrier heights to desired accuracy, and basis set and electron correlation effects were considered separately. The structures of the staggered and eclipsed conformations were optimized at the MP2/6-31G(*d*) level. Table III suggests that correlation effects beyond MP2 are small. Note that the 6-311G(*d,p*) basis set performs quite poorly in this case, overestimating the barrier

TABLE III. Internal rotation barrier of methanol ( $\text{kJ mol}^{-1}$ ). Electron correlation effects.<sup>a</sup>

	6-311G( <i>d,p</i> )	6-311+G(2 <i>df,p</i> )
RHF	5.28	4.24
MP2	6.13	4.45
MP3	5.86	4.37
MP4	6.09	4.41
QCISD	5.90	4.35
CCSD	5.89	4.37
QCISD(T)	6.02	4.39
CCSD(T)	6.01	4.40
QCISD[T]	6.03	4.35
CCSD[T]	6.02	4.38
Expt. <sup>b</sup>	4.466(4)	

<sup>a</sup>Frozen-core energy differences calculated using MP2/6-31G(*d*) structures.<sup>b</sup>Reference 54.

height by about  $1.5 \text{ kJ mol}^{-1}$ . Selecting the MP2 level of correlation, eleven basis sets were tested (Table IV). The barrier height as determined spectroscopically will contain zero-point vibrational energy (ZPVE) contributions from all other vibrational modes; Bell<sup>54</sup> estimated this effect for methanol to be  $+0.28 \text{ kJ mol}^{-1}$  using MP2/DZ(*d,p*) theory, which we expect to be typical. While it would be essential to include the ZPVE effect if *spectroscopic* accuracy is desired, it is not of concern when attempting to compute the entropy to a *thermodynamic* accuracy of  $1 \text{ J mol}^{-1} \text{ K}^{-1}$ , as demonstrated above with the data in Table II. For methanol, the use of the 6-311+G(2*df,p*) basis set (without ZPVE) provides an estimate ( $4.45 \text{ kJ mol}^{-1}$ ) within  $0.3 \text{ kJ mol}^{-1}$  of both the experimental and classical barrier heights ( $4.47$  and  $4.19 \text{ kJ mol}^{-1}$ , respectively). This is the ultimate basis set which is approximated in G1 theory,<sup>55</sup> and it was chosen in conjunction with MP2 theory (and without ZPVE) for barrier-height computation in this work. In the recent work of

TABLE IV. Internal rotation barrier of methanol ( $\text{kJ mol}^{-1}$ ). Basis set effects.<sup>a</sup>

	Number of basis functions	Barrier height
6-31G( <i>d</i> )	38	6.21
cc-pVDZ	48	6.34
6-311+G( <i>d</i> )	56	5.16
6-311G( <i>d,p</i> )	60	6.13
6-31+G( <i>d,p</i> )	62	5.08
aug-cc-pVDZ	82	4.73
6-31+G(2 <i>df,p</i> )	84	4.79
6-311+G(2 <i>df,p</i> )	92	4.45
6-31+G(3 <i>df,2p</i> )	108	4.43
6-311+G(3 <i>df,2p</i> )	114	4.21
cc-pVTZ	116	4.73
Expt. <sup>b</sup>	4.466(4)	
Expt. <sup>b</sup> (classical) <sup>c</sup>	4.19	

<sup>a</sup>MP2 frozen-core energy differences calculated using MP2/6-31G(*d*) structures.<sup>b</sup>Reference 54.<sup>c</sup>Using the MP2/DZ(*d,p*) back-correction of Ref. 54 to remove zero-point vibrational effects of other modes.

Chung-Phillips and Jebber,<sup>56</sup> an analysis of the effect of basis set on computed internal rotation barriers is provided for a series of small molecules, and supports our use of a large basis set with MP2 theory.

For more complicated internal rotation potentials, tabulated or fitted results based on the single cosine represent the only means of incorporating hindrances to free rotation without having to perform numerical integration. Therefore it becomes useful to be able to mimic each internal rotation with a single cosine term unless very high accuracy (better than  $1 \text{ J mol}^{-1} \text{ K}^{-1}$ ) is desired. The varying barrier heights in more complex one-dimensional rotations can be averaged, with “minor” barriers (of a height less than a quarter of the largest barrier height encountered during the rotation) being neglected. For multiple coupled internal rotations, the difficulty in selection of single-rotor potentials and the resulting errors produced by this approximation both increase with the magnitude of the coupling. Choosing the single-rotor barriers as the differences between standard conformations (staggered-staggered and staggered-eclipsed, for example) may result in high entropy estimates if there is a significant drop in the torsional potential energy at nonstandard conformations. Choosing the single-rotor barriers as the differences between true global minima and single-rotor maxima can be unsuitable in cases where the connection between a minimum and corresponding maximum on the true potential surface either (i) involves a change in the primary torsional coordinate which is substantially different from that in the idealized cosine potential (e.g.,  $40^\circ$  instead of  $60^\circ$  for a methyl rotation), or (ii) requires strong and nonuniform dependence of the secondary torsional coordinate upon the primary one. In this work, we use the latter approach, the single rotor barriers for the simple cosine models being chosen as differences between true global minima and single-rotor maxima. In the cases where this choice becomes poor, the potential will be sufficiently complex that a numerical integration will be required, and a full coupled potential should then be used, as we will demonstrate for  $(\text{CH}_3)_2\text{CH}^+$  in Sec. III C below.

Table V presents the calculated torsional barriers for a wide selection of molecules, to be used later in the paper in determining third-law entropies. The barriers to the internal rotation in  $\text{CH}_5^+$ , toluene, the *ortho*- and *para*-protonated toluenes, and the tertiary-butyl cation are deemed sufficiently small that we treat the rotations as free rotors in the entropy calculations. For example, for toluene and its *para*-protonated cation, the MP2/6-31G(*d*) methyl rotation barriers are  $0.22$  and  $0.21 \text{ kJ mol}^{-1}$ , respectively. For the tertiary-butyl cation, our conformational analysis (similar to an earlier one by Sieber *et al.*<sup>57</sup>) drew us to the conclusion that, although the potential surface for the torsional motions of the three methyl groups is qualitatively complex, it is quantitatively rather flat, fitting entirely within a  $\sim 6 \text{ kJ mol}^{-1}$  span. We shall comment on this species later, in Sec. VI D.

It can be seen from Table V that the effect of MP2 correlation for methyl rotation barriers is most significant for those cases where methyl groups are bonded to oxygen atoms or double-bonded systems. The importance of the larger basis set is substantial (greater than  $0.8 \text{ kJ mol}^{-1}$ ) when lone

TABLE V. Torsional barriers ( $\text{kJ mol}^{-1}$ ) calculated using MP2/6-31G(*d*) structures.

	MP2/ 6-31G( <i>d</i> )	HF/ 6-311+G(2 <i>df</i> , <i>p</i> )	MP2/ 6-311+G(2 <i>df</i> , <i>p</i> )	Experiment <sup>a</sup>
CH <sub>3</sub> -OH	6.21	4.24	4.45	4.5 <sup>d</sup>
CH <sub>3</sub> -NH <sub>2</sub>	10.72	8.52	8.57	8.2 <sup>e</sup>
CH <sub>3</sub> -SH	6.19	5.62	5.27	5.3 <sup>f</sup>
CH <sub>3</sub> -OCHO	4.55	5.16	5.28	4.9 <sup>g</sup>
CH <sub>3</sub> -CH <sub>2</sub> CN	13.88	13.88	13.41	
CH <sub>3</sub> -CHO	4.13	5.23	4.69	4.9 <sup>g</sup>
CH <sub>3</sub> -H <sub>2</sub> <sup>+</sup>	0.47	0.20	0.57	
CH <sub>3</sub> -CHCH <sub>2</sub>	8.18	9.27	8.44	8.2 <sup>h</sup>
CH <sub>3</sub> -CHCH <sub>3</sub> <sup>+</sup>	4.88 <sup>b</sup>	4.60 <sup>b</sup>	6.60 <sup>b</sup>	
CH <sub>3</sub> -OCH <sub>3</sub>	12.12	9.63	11.13	11.0, <sup>i</sup> 10.8 <sup>d</sup>
CH <sub>3</sub> -NHCH <sub>3</sub>	15.35	12.99	13.67	13.7 <sup>i</sup>
CH <sub>3</sub> -SCH <sub>3</sub>	8.86	9.04	8.98	8.7 <sup>i</sup>
CH <sub>3</sub> -C(O)CH <sub>3</sub>	3.17	2.86	2.61	3.5, <sup>i</sup> 3.3, <sup>d</sup> 2.8 <sup>j</sup>
CH <sub>3</sub> -C(OH)CH <sub>3</sub> <sup>+</sup> [ <i>trans</i> ]	1.47 <sup>b</sup>	1.46 <sup>b</sup>	2.00 <sup>b</sup>	
CH <sub>3</sub> -C(OH)CH <sub>3</sub> <sup>+</sup> [ <i>cis</i> ]	1.49 <sup>b</sup>	1.77 <sup>b</sup>	2.18 <sup>b</sup>	
CH <sub>3</sub> -CH <sub>2</sub> NH <sub>2</sub>	16.60	15.83	15.42	
NH <sub>2</sub> -CH <sub>2</sub> CH <sub>3</sub>	11.53 <sup>c</sup>	9.12 <sup>c</sup>	9.11 <sup>c</sup>	
CH <sub>3</sub> -C(CH <sub>2</sub> )CH <sub>3</sub>	9.47	10.09	9.25	8.9 <sup>i</sup>
CH <sub>3</sub> -N(CH <sub>3</sub> ) <sub>2</sub>	19.75	16.92	18.52	18.5 <sup>i</sup>
CH <sub>3</sub> -NH(CH <sub>3</sub> ) <sub>2</sub> <sup>+</sup>	14.36	14.46	14.24	

<sup>a</sup>Experimental values include ZPVE effects from the other vibrational modes.

<sup>b</sup>For these systems, the stationary points used in computing the barrier heights here do not correspond to "idealized" conformations. See the text.

<sup>c</sup>These are averages of the differing barrier heights encountered during -NH<sub>2</sub> rotation.

<sup>d</sup>Chao *et al.* (Ref. 58).

<sup>e</sup>Takagi and Kojima (Ref. 59).

<sup>f</sup>Sastry *et al.* (Ref. 60).

<sup>g</sup>Fateley and Miller (Ref. 61).

<sup>h</sup>Włodarczyk *et al.* (Ref. 62).

<sup>i</sup>Fateley and Miller (Ref. 63).

<sup>j</sup>Kundu *et al.* (Ref. 64).

pairs are present. The MP2/6-311+G(2*df*,*p*) barriers agree with experimental values<sup>58-64</sup> to within  $0.4 \text{ kJ mol}^{-1}$  for all species. The agreement with the Rydberg-jet-based result for acetone ( $2.8 \text{ kJ mol}^{-1}$ )<sup>64</sup> is particularly satisfying, because the traditional longstanding experimental values for acetone ( $3.47-3.48 \text{ kJ mol}^{-1}$  from far IR vibrational transitions,<sup>63,65</sup> and  $3.17-3.28$  from microwave rotational splittings using independent-rotor models<sup>65-69</sup>) have been substantially higher, as have many *ab initio* results using smaller basis sets.<sup>70-75</sup> The high degree of potential coupling of the two methyl rotors in acetone is apparently responsible for causing greater difficulties in understanding the nature of the internal rotations in this case.

For internal rotor moments of inertia, the MP2/6-31G(*d*) structures were deemed to be suitable, based on the results for overall rotational entropy. However, internal moments of inertia can be approximated in many ways, and this subject warranted a separate investigation in itself.

## B. Levels of approximation for internal moments of inertia

Research into the energy levels and thermodynamic properties of internal rotations was most prevalent in the 1930s and 40s. After initial contributions by such scientists as Nielsen,<sup>76</sup> Mayer *et al.*,<sup>77</sup> Teller,<sup>78</sup> Kassel,<sup>79-82</sup> Pitzer,<sup>83</sup> and Wilson, Jr.,<sup>84,85</sup> generalization of the theories as applied

to thermodynamic properties was established principally by Pitzer and co-workers.<sup>45-47</sup> The important connection with spectroscopic theory for the energy levels of internal rotations was solidified in the early 1950s with the advances of Dennison and co-workers,<sup>86-88</sup> whose meticulous work on the microwave and infrared spectra of methanol provided a substantially improved picture of a hindered rotation, and one which afforded agreement between the calorimetric and spectroscopic thermodynamics which were studied in concert by the Pitzer group.<sup>89,90</sup>

As far as thermodynamic properties are concerned, the theory rests upon the numerical solutions of the Matthieu equations, which result from the one-dimensional Schrödinger equation for a rotor having moment of inertia *I* and the cosine potential in Eq. (3). The first extension to the general case of a multi-rotor vibrating molecule simply uses the independent-rigid-rotor assumption. More accurate extensions require more elaborate expressions for the potential energy for internal rotations, together with numerical integration and further approximation. While the theory with the independent-rigid-rotor model cannot consider potential coupling, it can account for kinetic (angular momentum) coupling approximately via a series of reductions of the internal moments of inertia. These reductions and various approximations are now summarized and investigated.

The notation  $I^{(m,n)}$  is introduced here as a means of

bookkeeping the various approximations of an internal moment of inertia. Here the  $n$  indicates the level of approximation for a rotor attached to a fixed frame before any reduction of this moment of inertia due to coupling with external or other internal rotations, while the  $m$  indicates the level of approximation of the coupling reduction. Since one can arbitrarily choose either end ('left' or 'right') of the twisting bond to be the rotating group, a subscript  $L$  or  $R$  can be added in most cases, i.e.  $I_L^{(m,n)}$  and  $I_R^{(m,n)}$ , which can produce different values for some approximations although they will be identical in an exact treatment.

If  $n=1$ , the moment of inertia of the rotating group is computed about the axis containing the twisting bond. If  $n=2$ ,  $I$  is computed about the axis parallel to the bond but passing through the center-of-mass of the rotating group.<sup>91</sup> If  $n=3$ ,  $I$  is computed about the axis passing through the centers-of-mass of both the rotating group and the remainder of the molecule.

If  $m=1$ , the moment of inertia of the rotating group is not reduced. If  $m=2$ , the reduced moment due to coupling with overall molecular rotation is approximated<sup>91</sup> by

$$1/I^{(2,n)} = 1/I_L^{(1,n)} + 1/I_R^{(1,n)}. \quad (4)$$

If  $m=3$ , the coupling with molecular rotation is properly performed<sup>45</sup> with

$$I_X^{(3,n)} = I_X^{(1,n)} - \Lambda_{XX}^{(n)}, \quad (5)$$

$$\Lambda_{XX}^{(n)} = I_X^{(1,n)^2} (\lambda_{X1}^2/I_1 + \lambda_{X2}^2/I_2 + \lambda_{X3}^2/I_3) \quad \text{for } n < 4. \quad (6)$$

where the  $I_i$  are the principal moments of inertia of the molecule, and  $\lambda_{Xi}$  is the direction cosine between the  $i$ th principal axis and the axis of twisting about which  $I_X^{(1,n)}$  was computed.

The  $I_X^{(3,1)}$  estimator is exact for molecules with a single, symmetric rotor. For a single asymmetric rotor (and, if one wished, for instantaneously asymmetric methyl rotors such as those resulting from equilibrium structures), there is an exact  $I_X^{(3,4)}$  estimator, with a  $\Lambda_{XX}^{(4)}$  correction in Eq. (5) which is more complex than that of Eq. (6), and the reader is referred to the original work for details.<sup>46</sup>

For molecules with multiple rotors, individual reduced moments of inertia for each internal rotation mode are not easily defined. The crude approximation of Pitzer and Gwinn<sup>45</sup> is a further reduction for the case of multiple rotors attached to the same rigid frame, and we denote it as  $m=4$ ; here the kinetic coupling of one internal rotation (identified by a chosen rotating group  $X$ ) with other internal rotations (identified by their chosen rotating groups  $Y$ ) is incorporated using

$$I_X^{(4,n)} = I_X^{(3,n)} - 0.5 \sum \Lambda_{XY}^{(n)^2} / I_Y^{(3,n)}, \quad (7)$$

$$\Gamma_{XY}^{(n)} = I_X^{(1,n)} I_Y^{(1,n)} (\lambda_{X1} \lambda_{Y1} / I_1 + \lambda_{X2} \lambda_{Y2} / I_2 + \lambda_{X3} \lambda_{Y3} / I_3) \quad \text{for } n < 4, \quad (8)$$

where the sum in Eq. (7) is over all  $Y$ . Just as with  $\Lambda_{XX}^{(4)}$ , the more complex formula for  $\Lambda_{XY}^{(4)}$  can be found elsewhere.<sup>46</sup>

TABLE VI. Approximations for the internal moment of inertia ( $\text{amu } \text{\AA}^2$ ).<sup>a</sup>

	Methanol		Dimethylether	
	-CH <sub>3</sub>	-OH	-CH <sub>3</sub>	-OCH <sub>3</sub>
$I^{(1,1)}$	3.1794	0.8635	3.2072	31.2002
$I^{(1,2)}$	3.1790	0.8123	3.2071	17.1350
$I^{(1,3)}$	3.1842	0.7910	3.0947	12.0185
$I^{(2,1)}$		0.6790		2.9083
$I^{(2,2)}$		0.6470		2.7015
$I^{(2,3)}$		0.6336		2.4610
$I^{(3,1)}$	0.6402	0.6762	2.6094	-25.3738
$I^{(3,2)}$	0.6405	0.6465	2.6093	0.0714
$I^{(3,3)}$	0.6318	0.6335	2.3946	1.4595
$I^{(3,4)}$	0.6348	0.6348	2.5978	2.5978
$I^{(4,1)}$			2.5678	
$I^{(4,2)}$			2.5677	
$I^{(4,3)}$			2.2982	
$I^{(4,4)}$			2.5559	

<sup>a</sup>These were computed using structural data for the optimized MP2/6-31G( $d$ ) minimum for each species. See the text for  $I^{(m,n)}$  notation.

This approximation arises from deliberate neglect of the angular momentum cross terms  $P_X P_Y$  in the total kinetic energy expression, and the accuracy of such an omission for thermodynamic purposes is unknown. To cover the general case, including rotors within other rotors, an ultimate treatment is the determinant method of Kilpatrick and Pitzer,<sup>47</sup> which we could designate an  $m=5$  treatment; however, the treatment is laborious and requires an extra scaling approximation to incorporate the angular momentum cross terms, and considering the probable errors which persist regardless due to nonrigid rotations and minor inaccuracies in equilibrium structures, we chose not to examine it.

Table VI presents the results of these approximations for the internal rotation of methanol and one of the (equivalent) internal rotations of dimethylether. The structural parameters of the MP2/6-31G( $d$ ) optimized geometries were used, which results in instantaneous asymmetric structures for the methyl groups, due to differing C-H bond lengths and  $\angle\text{OCH}$  angles within each group at the optimized minima. However, the effect of methyl group asymmetry is small, as seen in comparing the  $n=1$  and  $n=2$  results using the methyl rotors. Also, treating the methyl groups as the rotors, rather than the asymmetric hydroxy and methoxy groups, allows the simpler  $n=1$  estimates to be used without great loss of accuracy. As stated before, the  $I_X^{(3,4)}$  computation is exact (within the rigid-rotor approximation) for molecules with a single internal rotation, and hence the  $I_L^{(3,4)}$  and  $I_R^{(3,4)}$  values are equal since the exact result should be independent of the choice of the rotating group. There are  $I_{\text{CH}_3}^{(4,n)}$  but no  $I_{\text{OCH}_3}^{(4,n)}$  values for dimethylether because the  $m=4$  approximation requires a common fixed frame for the two rotating groups.

For methanol, the desired value of  $0.6348 \text{ amu } \text{\AA}^2$  can be approximated to within 2% ( $0.015 \text{ amu } \text{\AA}^2$ ) by  $I_{\text{CH}_3}^{(3,1)}$ ,  $I^{(2,2)}$  and  $I^{(2,3)}$ , and within 7% by  $I_{\text{OH}}^{(3,1)}$  and  $I^{(2,1)}$ . For dimethylether, the asymmetric methoxy group produces disastrous re-

TABLE VII. Calculated internal moments of inertia ( $\text{amu } \text{\AA}^2$ ).<sup>a</sup>

	$I^{(1,1)}$	$I^{(2,1)}$	$I^{(3,1)}$	$I^{(4,1)}$
Single rotors				
CH <sub>3</sub> -OH	3.1794	0.6790	0.6402	
CH <sub>3</sub> -OH <sub>2</sub> <sup>+</sup>	3.3031	1.0989	1.0763	
CH <sub>3</sub> -NH <sub>2</sub>	3.1505	1.1675	1.1360	
CH <sub>3</sub> -SH	3.1716	1.1424	1.1172	
CH <sub>3</sub> -C <sub>6</sub> H <sub>5</sub>	3.1509	3.0425	3.0424	
CH <sub>3</sub> -CH <sub>2</sub> CN	3.1659	3.0767	2.8661	
CH <sub>3</sub> -CHO	3.1992	2.7012	2.2023	
H <sub>2</sub> -CH <sub>3</sub> <sup>+</sup>	0.4521	0.3978	0.3977	
Multiple rotors				
CH <sub>3</sub> -OCH <sub>3</sub>	3.2072	2.9082	2.6094	2.5678
CH <sub>3</sub> -C(O)CH <sub>3</sub>	3.1902	2.9989	2.9965	2.9949
CH <sub>3</sub> -C(OH)CH <sub>3</sub> <sup>+</sup> [ <i>trans</i> ] <sup>b</sup>	3.2080	3.0169	3.0161	3.0139
CH <sub>3</sub> -C(OH)CH <sub>3</sub> <sup>+</sup> [ <i>cis</i> ] <sup>b</sup>	3.1901	3.0001	2.9993	2.9971
CH <sub>3</sub> -CH <sub>2</sub> NH <sub>2</sub>	3.1616	2.8986	2.6649	2.5788
NH <sub>2</sub> -CH <sub>2</sub> CH <sub>3</sub>	1.8692	1.7768	1.3357 <sup>c</sup>	1.2926 <sup>c</sup>
CH <sub>3</sub> -C(CH <sub>3</sub> ) <sub>2</sub> <sup>+</sup> [ <i>up</i> ] <sup>d</sup>	3.1997	3.0328	3.0327	3.0305
CH <sub>3</sub> -C(CH <sub>3</sub> ) <sub>2</sub> <sup>+</sup> [ <i>down</i> ] <sup>d</sup>	3.1957	3.0271	3.0271	3.0247

<sup>a</sup>These were computed using the optimized structure of the lowest MP2/6-31G(*d*) minimum for each species. See the text for  $I^{(m,n)}$  notation.

<sup>b</sup>See Fig. 1.

<sup>c</sup>These values are  $I^{(3,4)}$  and  $I^{(4,4)}$  for the more imbalanced-NH<sub>2</sub> group.

<sup>d</sup>See Fig. 2.

sults unless  $n=4$ , while the results for the methyl group behave well for  $n<4$  and indicate that rotor-rotor coupling ( $m=4$ ) is important. The  $I_{\text{CH}_3}^{(3,1)}$  estimate is 2% too high, while the  $I^{(2,2)}$  and  $I^{(2,3)}$  estimates are 4–6% high and  $I^{(2,1)}$  is 14% too high.

Table VII presents, for several different internal rotations, the calculated moments of inertia using the approximations we deemed most eligible for use in the general utility procedures E1, E2, and E3. As written, the groups on the left are taken to be the rotating groups for the purposes of computation. The basic  $I^{(1,1)}$  values for methyl groups cluster tightly about  $3(1.0078)(1.09 \sin 109.5^\circ)^2 = 3.19 \text{ amu } \text{\AA}^2$ . The methyl groups in protonated acetone (*cis* and *trans* to the OH group, see Fig. 1) and at the optimized minimum of the tertiary-butyl cation (Fig. 2) are nonequivalent, and hence are listed separately. The improvements from  $I^{(1,1)}$  to  $I^{(3,1)}$  are most significant when the chosen rotating group is the heavier of the two ends. When the chosen rotating group is the lighter of the two ends, the  $I^{(1,1)}$  approximation lies within 50% (and often within 20%) of the  $I^{(3,1)}$  and  $I^{(4,1)}$  values. The improvements from  $I^{(2,1)}$  to  $I^{(3,1)}$  are most significant for molecules having groups with large mass asymmetry with respect to the internal rotation axis, such as ethyl or aldehyde groups, and  $I^{(2,1)}$  significantly improves upon the lighter-end  $I^{(1,1)}$  values when the two ends of the molecule are evenly matched in mass. The data in Table VII show that  $I^{(2,1)}$  generally lies within 5% of the best values, although in the small number of cases where there is large mass asymmetry the error can be as large as 30%.

The rightmost entries in Table VII, using the  $I^{(3,1)}$  approximation for single-rotor molecules and  $I^{(4,1)}$  for multirotor molecules (or  $I^{(3,4)}$  and  $I^{(4,4)}$  respectively if an asymmetric rotor is involved), are the values used in determining

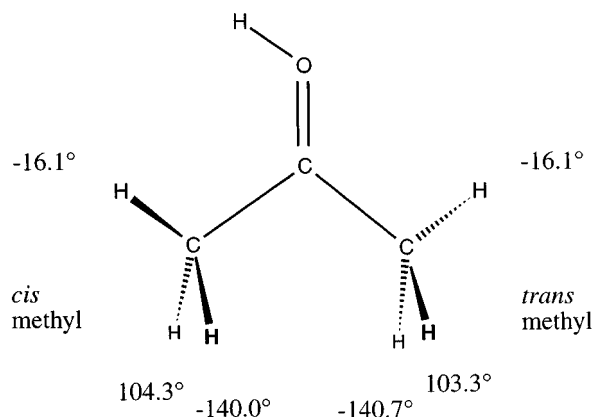


FIG. 1. Optimized conformation ( $C_1$  symmetry) of protonated acetone,  $(\text{CH}_3)_2\text{COH}^+$ . Numbers indicate MP2/6-31G(*d*) H-C-C-O torsional angles, in degrees from a *cis* conformation.

entropies in Section IV and for the E2 and E3 models (see Sec. V). It was only necessary to employ  $I^{(4,4)}$  once, for the ethyl-NH<sub>2</sub> internal rotation in ethylamine, in the present study. For the simpler E1 model,  $I^{(2,1)}$  was chosen instead, as it has the possibility of being more efficiently computed on a regular basis.

### C. Selection of potential functions for rotor-rotor coupling

Effects of rotor-rotor potential coupling became apparent in many cases. One manifestation of this is in the location of minima on the MP2/6-31G(*d*) potential energy surfaces. Two examples of more complex situations occur with the protonated cations of propene and acetone,  $(\text{CH}_3)_2\text{CH}^+$  and  $(\text{CH}_3)_2\text{COH}^+$ , whose minimum energy conformations involve methyl rotor positions which are conrotationally distorted from idealized and more symmetrical  $C_{2v}$  and  $C_s$  structures, respectively. In these cases, even the single-rotor potentials become more difficult to represent with simple cosine potentials (as required by the Pitzer tables). The second manifestation of rotor-rotor potential coupling is in the

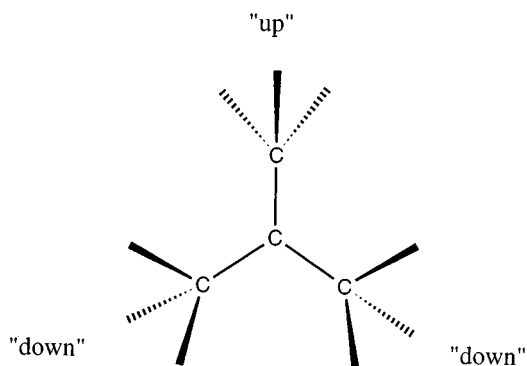


FIG. 2. Optimized conformation ( $C_s$  symmetry) of *t*-butyl cation,  $(\text{CH}_3)_3\text{C}^+$ . The carbon framework is slightly puckered after optimization.

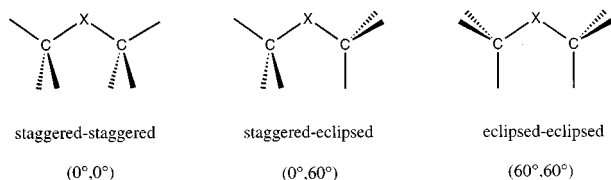


FIG. 3. The three idealized conformations of (1,1)-dimethyl systems.

increased error associated with the independent-rotor assumption. In some cases, the energy of the single-rotor maximum (e.g. eclipsed-staggered, see Fig. 3) was found to be significantly different from the average of energies of the minimum (e.g. staggered-staggered) and the two-rotor double-maximum (e.g. eclipsed-eclipsed), which would not be the case if the rotors were independent.

In calculating thermodynamic properties of internal rotation modes, the simplest strategy which incorporates hindered rotor potentials involves keeping the independent-mode approximation, ignoring the complexities in the one-dimensional potential surfaces, and using the Pitzer tables individually for each rotation. This will correspond to our E2 procedure in Sec. V. The required barrier heights for systems with two coupled rotors were computed as the differences in energy between the global minima and single-rotor maxima conformations. These are the barriers displayed in Table V. The alternative use of energies of idealized high-symmetry optimized conformations for  $(\text{CH}_3)_2\text{CH}^+$  and  $(\text{CH}_3)_2\text{COH}^+$  would result in barrier heights which are 2.6 and 0.6  $\text{kJ mol}^{-1}$  lower than the values in Table V, which are substantial differences (39% and 29% reductions, respectively).

For more complex potentials, Pitzer and Gwinn<sup>45</sup> proposed the following approximation ( $Q_{\text{Scaled}}$ ) to the quantum mechanical canonical partition function  $Q_{\text{Quant}}$ :

$$Q_{\text{Scaled}} = Q_{\text{Class}} [Q_{\text{HO Quant}} / Q_{\text{HO Class}}], \quad (9)$$

where the classical partition function ( $Q_{\text{Class}}$ ) is scaled by the ratio suitable for converting the classical partition function for a harmonic oscillator ( $Q_{\text{HO Class}}$ ) to its quantum mechanical result ( $Q_{\text{HO Quant}}$ ).<sup>45</sup> Use of this approximation requires a (possibly numerical) solution of multidimensional integrals of the form

$$P(m) = \int \cdots \int (V/kT)^m e^{-(V/kT)} d\alpha_1 \cdots d\alpha_n, \quad (10)$$

where the complexity of the coupled  $n$ -rotor potential  $V(\alpha_1, \dots, \alpha_n)$  naturally affects the complexity of the integration. We tested this approximation (just as Pitzer and Gwinn did) with the one-dimensional cosine potential, using up to 50-point Gauss–Legendre quadrature between 0 and  $2\pi/\sigma$  (where  $\sigma$ , the periodicity of the cosine, was taken to be 3), yielding the results shown in Table VIII. In the numerical integration, 10-point quadrature was sufficient to converge the entropies to  $0.01 \text{ J mol}^{-1} \text{ K}^{-1}$ , while 20-point quadrature was sufficient for  $0.001 \text{ J mol}^{-1} \text{ K}^{-1}$  convergence (and was used exclusively in ensuing calculations for each dimension). Table VIII is presented in the same format as Pitzer and

TABLE VIII. Error in hindered rotor entropy ( $\text{J mol}^{-1} \text{ K}^{-1}$ , at 1 atm and 298.15 K) due to the use of Pitzer and Gwinn's approximate partition function,  $Q_{\text{Scaled}}$ .

$V_0/RT$	$S_{\text{Scaled}} - S_{\text{exact}}$		
	$1/Q_f = 0.20$	$1/Q_f = 0.30$	$1/Q_f = 0.40$
1	+0.016	+0.049	+0.094
4	-0.003	-0.008	+0.010
9	-0.003	-0.002	-0.010
16	+0.012	-0.005	-0.068

Gwinn's<sup>45</sup> Table VIII (although they used  $\text{cal mol}^{-1} \text{ K}^{-1}$  units) and confirms that errors in entropy due to this approximation are less than  $0.1 \text{ J mol}^{-1} \text{ K}^{-1}$  for the range of rotors and temperatures considered here. We could not reproduce their test results beyond  $0.1 \text{ J mol}^{-1} \text{ K}^{-1}$  accuracy, presumably due to differences in numerical integration and values of fundamental constants. Nonetheless, the approximation is sufficiently good to allow us to perform statistical thermodynamics using more complex, coupled-potential forms, to the accuracy of the *ab initio* level of theory used for the molecular parameters themselves, and will be incorporated into our E3 procedure of Sec. V.

The most general Fourier series potential for a two-rotor system is

$$\begin{aligned}
 V(\alpha_1, \alpha_2) = & \sum_{K=0}^{\infty} \sum_{L=0}^{\infty} [A_{KL}^{cc} \cos n_1 K \alpha_1 \cos n_2 L \alpha_2 \\
 & + A_{KL}^{ss} \sin n_1 K \alpha_1 \sin n_2 L \alpha_2 \\
 & + A_{KL}^{cs} \cos n_1 K \alpha_1 \sin n_2 L \alpha_2 \\
 & + A_{KL}^{sc} \sin n_1 K \alpha_1 \cos n_2 L \alpha_2], \quad (11)
 \end{aligned}$$

where  $n_1$  and  $n_2$  are symmetry numbers for the internal rotations, e.g., 3 for methyl groups and 1 for the ethyl- $\text{NH}_2$  torsion in ethylamine. The initial work on rotor-rotor potentials in the late 1950s focussed on dimethyl systems having a  $C_{2v}$  frame, and this general form of  $V(\alpha_1, \alpha_2)$  was first proposed for dimethyl systems ( $n_1 = n_2 = 3$ ) by Grant *et al.*<sup>92</sup> in 1970 (ignoring a factor of 2 in the coefficients), although Fourier expansions were certainly employed earlier for such systems. If the Fourier series is expanded about a  $C_{2v}$  position denoted  $\alpha_1 = \alpha_2 = 0$ , then Eq. (11) reduces to

$$\begin{aligned}
 V(\alpha_1, \alpha_2) = & \sum_{K=0}^{\infty} \sum_{L=0}^{\infty} [A_{KL}^{cc} \cos 3K \alpha_1 \cos 3L \alpha_2 \\
 & + A_{KL}^{ss} \sin 3K \alpha_1 \sin 3L \alpha_2] \quad (12)
 \end{aligned}$$

with the additional symmetries  $A_{KL}^{cc} = A_{LK}^{cc}$  and  $A_{KL}^{ss} = A_{LK}^{ss}$ . This form was also presented by Grant *et al.*<sup>92</sup> and is used (without the factor of 2) in the recent works of Senent, Moule, and Smeyers.<sup>75,93,94</sup> With alternative choices for sign and notation conventions, the  $A_{00}^{cc}$  constant term, and occa-

sional factors of 2, the first few terms of Eq. (11) have been used by Groner and Durig<sup>95,96</sup> and, earlier, in the seminal work by Swalen and Costain.<sup>66</sup>

If we ignore the higher terms above  $K+L=2$  in Eq. (11), then

$$\begin{aligned} V(\alpha_1, \alpha_2) = & A_{00}^{cc} + A_{10}^{cc} \cos n_1 \alpha_1 + A_{01}^{cc} \cos n_2 \alpha_2 \\ & + A_{20}^{cc} \cos 2n_1 \alpha_1 + A_{02}^{cc} \cos 2n_2 \alpha_2 \\ & + A_{11}^{cc} [\cos n_1 \alpha_1 \cos n_2 \alpha_2] \\ & + A_{11}^{ss} [\sin n_1 \alpha_1 \sin n_2 \alpha_2], \end{aligned} \quad (13)$$

which is the seven-term potential we generally began with (and usually simplified). The seven parameters can physically be thought of in the following way: an energy zero, two individual barrier amplitudes, two additional parameters to account for complexities in the one-dimensional methyl rotations (e.g., minima distorted from maximally symmetric positions), and two coupling amplitudes. The two coupling amplitudes may in turn be thought of as describing firstly the relative preference for conrotatory vs disrotatory motion ( $A_{11}^{ss}$  term), and secondly the relative height of the double maximum above or below the level of the sum of the two single maxima ( $A_{11}^{cc}$  term).

In the majority of our cases we have equivalent methyl rotors and  $C_{2v}$  minima [such as in  $(\text{CH}_3)_2\text{CO}$ ] for which we employ the three-parameter function

$$\begin{aligned} V(\alpha_1, \alpha_2) = & A_{00}^{cc} + A_{10}^{cc} \cos 3\alpha_1 + A_{10}^{cc} \cos 3\alpha_2 \\ & + A_{11}^{cc} [\cos 3\alpha_1 \cos 3\alpha_2] \\ & - |A_{11}^{cc}| [\sin 3\alpha_1 \sin 3\alpha_2], \end{aligned} \quad (14)$$

where we drop the  $A_{20}^{cc}$  and  $A_{02}^{cc}$  terms for simplicity, equate  $A_{01}^{cc}$  and  $A_{10}^{cc}$  due to symmetry, and approximate  $A_{11}^{ss}$  with  $-|A_{11}^{cc}|$ . The  $A_{11}^{ss}$  assumption has been used before<sup>92</sup> and has support (see Reference 65). This allows us to obtain a qualitatively correct and quantitatively accurate potential function from the three energies obtained at the three obvious (and optimized) stationary points represented in Figure 3. Using the usual convention, we define the  $\alpha_1$  and  $\alpha_2$  torsions to be describing conrotation if they increase concomitantly; hence the selection of  $A_{11}^{ss}$  to be  $-|A_{11}^{cc}|$  causes incremental conrotation to rise in energy more slowly than disrotation (which is found to hold in all our cases from the HF frequency analyses). The sign of  $A_{11}^{ss}$  does not affect the total molecular entropy. The  $(0^\circ, 0^\circ)$  origin is taken to be the staggered-staggered conformation since that is most often the location of the global minimum.

The quantity  $V_{12}=4 A_{11}^{cc}$  is the energy difference between the double maximum [e.g.  $V(60^\circ, 60^\circ)$  for dimethyl systems if  $V(0^\circ, 0^\circ)$  is chosen to be 0] and the sum of the two single rotor maxima  $V_L + V_R$  [e.g.,  $V(60^\circ, 0^\circ) + V(0^\circ, 60^\circ)$  for dimethyl systems]. Ratios of  $V_{12}$  to  $V_L + V_R$  using MP2/6-311+G(2df,p) energies and MP2/6-31G(d) structures are:  $(\text{CH}_3)_2\text{NH}_2^+$  +0.15,  $(\text{CH}_3)_2\text{O}$  -0.09,  $(\text{CH}_3)_2\text{S}$  +0.01,  $(\text{CH}_3)_2\text{CCH}_2$  +0.15,  $(\text{CH}_3)_2\text{CO}$  +0.73,  $(\text{CH}_3)_2\text{CH}^+$  +0.83, and  $(\text{CH}_3)_2\text{COH}^+$  +1.66. Here the  $V_L$  and  $V_R$  for

TABLE IX. Effect of the  $V_{12}$  potential coupling magnitude on third-law entropy contributions ( $\text{J mol}^{-1} \text{K}^{-1}$ , at 1 atm and 298.15 K) from two equivalent internal rotation modes, using Pitzer and Gwinn's  $Q_{\text{scaled}}$  and normal-mode torsional frequencies from the model potential surface.<sup>a</sup>

$V_0$ ( $\text{kJ mol}^{-1}$ )	$S_{\text{coup}} - S_{\text{uncoup}}$			
	$V_{12} = -V_0/2$	$V_{12} = 0$	$V_{12} = V_0/2$	$V_{12} = V_0$
1.0	+0.06	0	-0.09	-0.19
4.0	+0.65	0	-0.67	-1.30
7.0	+1.05	0	-0.84	-1.51
10.0	+1.02	0	-0.69	-1.20
13.0	+0.84	0	-0.50	-0.82

<sup>a</sup>The results are identical to the digits reported for both  $I^{(4,1)}=2.5$  and  $3.0 \text{ amu } \text{\AA}^2$ .

$(\text{CH}_3)_2\text{CH}^+$  and  $(\text{CH}_3)_2\text{COH}^+$  necessarily correspond to the barriers obtained from idealized high-symmetry conformations.

The effect of the coupling of rotor potentials can be deduced in the following way. With our independent-rotor model, if two methyl group rotations in a molecule are equivalent, both having moment of inertia  $I_0$  and potential barrier  $V_0$ , then they both contribute the same amount  $S_0$  to the absolute entropy. If one symmetrizes the two rotors, then the symmetric and antisymmetric (conrotatory and disrotatory) combinations would each have moment of inertia  $2I_0$  and (in the absence of potential coupling) barrier height  $2V_0$ , which results in two identical contributions of  $S_0$  to the entropy, just as in the unsymmetrized case. Therefore, the symmetrized picture implies that if  $V_{12}$  is positive, the conrotatory and disrotatory modes would encounter a higher barrier ( $2V_0 + V_{12}$ ) and the true contributions to the entropy should be somewhat lower than what we would find by ignoring  $V_{12}$ . This result does in fact hold in each of our cases in which  $V_{12}$  is positive. This is dissimilar to the effect of kinetic coupling terms, which (as has been argued before<sup>45</sup>) will raise some energy levels and lower others. Hence the effects of neglecting kinetic coupling should be relatively small due to some cancellation of errors in the partition function.

To quantify the effect of the coupling term  $V_{12}$ , several calculations were performed on hypothetical dimethyl systems with varying rotor moments of inertia  $I_L^{(4,1)} = I_R^{(4,1)}$ , barrier heights  $V_0 = V_L = V_R$ , and coupling magnitudes  $V_{12}$ , using a rearranged form of the potential in Eq. (14) in conjunction with the approximate partition function  $Q_{\text{scaled}}$ . The torsional frequencies for use in  $Q_{\text{scaled}}$  were found via normal mode analysis to be

$$\omega_{\pm} = \frac{1}{2\pi} \sqrt{\frac{\frac{9}{2} V_0 \pm \frac{9}{4} V_{12}}{I_X^{(3,1)} \pm \Lambda_{XY}^{(1)}}} \quad (15)$$

and  $\Lambda_{xy}^{(1)}$  was chosen to be  $0.03 \text{ amu } \text{\AA}^2$ . The results are displayed in Table IX. The magnitude of the effect depends upon both the relative and absolute magnitude of the single barrier height  $V_0$ ; when  $V_{12} = V_0/2$ , the magnitude of entropy suppression due to potential coupling varies from 0 to more

TABLE X. Parameters for the two-dimensional potential functions used for systems with two internal rotation modes ( $\text{kJ mol}^{-1}$ ).<sup>a</sup>

	$A_{00}^{cc}$	$A_{10}^{cc}$	$A_{01}^{cc}$	$A_{20}^{cc}$	$A_{02}^{cc}$	$A_{11}^{cc}$	$A_{11}^{ss}$	$A_{03}^{cc}$
$(\text{CH}_3)_2\text{CH}^+$	6.2179	3.7138	$A_{10}^{cc}$	1.0829	$A_{20}^{cc}$	1.6838	-2.4164	...
$(\text{CH}_3)_2\text{O}$	10.6306	-5.0668	$A_{10}^{cc}$	...	...	-0.4970	$+A_{11}^{cc}$	...
$(\text{CH}_3)_2\text{OH}^+$	7.3804	-3.8280	$A_{10}^{cc}$	...	...	0.2756	$-A_{11}^{cc}$	...
$(\text{CH}_3)_2\text{NH}$	13.4189	-6.5850	$A_{10}^{cc}$	...	...	-0.2490	$+A_{11}^{cc}$	...
$(\text{CH}_3)_2\text{NH}_2^+$	12.8370	-6.8736	$A_{10}^{cc}$	...	...	-0.9101	$-A_{11}^{cc}$	...
$(\text{CH}_3)_2\text{S}$	9.0081	-4.5198	$A_{10}^{cc}$	...	...	0.0315	$-A_{11}^{cc}$	...
$(\text{CH}_3)_2\text{SH}^+$	9.5367	-5.0334	$A_{10}^{cc}$	...	...	0.5300	$-A_{11}^{cc}$	...
$(\text{CH}_3)_2\text{CO}$	3.5656	-2.2582	$A_{10}^{cc}$	...	...	0.9508	$-A_{11}^{cc}$	...
$(\text{CH}_3)_2\text{COH}^+$	2.6066	-1.9548	-2.0418	0.2638	0.2589	1.2492	-0.7864	...
$\text{CH}_3\text{CH}_2\text{NH}_2^b$	12.5434	-7.7192	0.7731	...	-0.2550	0.0108	$-A_{11}^{cc}$	-4.5608
$\text{CH}_3\text{CH}_2\text{NH}_3^+$	13.1775	-7.7425	-5.9975	...	...	0.5625	$-A_{11}^{cc}$	...
$(\text{CH}_3)_2\text{CCH}_2$	9.9243	-5.3017	$A_{10}^{cc}$	...	...	0.6792	$-A_{11}^{cc}$	...

<sup>a</sup>All PESs have minima at (0,0) except  $[\text{Me}_2\text{COH}]^+$  ( $17.25^\circ, 15.80^\circ$ ) and  $[\text{Me}_2\text{CH}]^+$  ( $38.71^\circ, 38.71^\circ$ ). The normal modes for ethylamine were computed at the ( $0^\circ, 121.56^\circ$ ) minimum.

<sup>b</sup>For ethylamine, the coupling terms (listed under  $A_{11}^{cc}$  and  $A_{11}^{ss}$ ) are  $A_{13}^{cc}$  and  $A_{13}^{ss}$ .

than  $0.8 \text{ J mol}^{-1} \text{ K}^{-1}$  (the effect peaking when  $V_0 \approx 7 \text{ kJ mol}^{-1}$ ), while if  $V_{12} = 5 \text{ kJ mol}^{-1}$  (cutting diagonally across the bottom right corner of the table), the suppression varies from less than 0.5 (high  $V_0$ ) to more than 1.3 (low  $V_0$ )  $\text{J mol}^{-1} \text{ K}^{-1}$ .

For  $(\text{CH}_3)_2\text{CH}^+$ , we employed the five-parameter potential,

$$\begin{aligned}
 V(\alpha_1, \alpha_2) = & A_{00}^{cc} + A_{10}^{cc} \cos n_1 \alpha_1 + A_{10}^{cc} \cos n_2 \alpha_2 \\
 & + A_{20}^{cc} \cos 2n_1 \alpha_1 + A_{20}^{cc} \cos 2n_2 \alpha_2 \\
 & + A_{11}^{cc} [\cos n_1 \alpha_1 \cos n_2 \alpha_2] \\
 & + A_{11}^{ss} [\sin n_1 \alpha_1 \sin n_2 \alpha_2], \quad (16)
 \end{aligned}$$

where we have equated  $A_{01}^{cc} = A_{10}^{cc}$  and  $A_{02}^{cc} = A_{20}^{cc}$  due to symmetry.

For  $(\text{CH}_3)_2\text{COH}^+$ , the full seven-parameter potential in Eq. (13) was employed (even though  $A_{01}^{cc} \approx A_{10}^{cc}$  and  $A_{02}^{cc} \approx A_{20}^{cc}$ ) with  $\alpha_1$  measuring the *trans*-methyl rotation (*trans* to OH) and  $\alpha_2$  the *cis*-methyl rotation, in order to be qualitatively correct.

For  $\text{CH}_3\text{CH}_2\text{NH}_3^+$ , we used a four-parameter potential ( $A_{00}^{cc}$ ,  $A_{01}^{cc}$ ,  $A_{10}^{cc}$ , and  $A_{11}^{cc}$ ) where  $\alpha_1$  denotes the methyl rotation and  $\alpha_2$  the  $\text{NH}_3$  rotation, approximating  $A_{11}^{ss}$  with  $-|A_{11}^{cc}|$  as in Eq. (14).

For  $\text{CH}_3\text{CH}_2\text{NH}_2$ , the Fourier series for the asymmetric internal rotation of  $\text{NH}_2$  versus  $\text{CH}_3\text{CH}_2$  has the periodicity parameter  $n_2 = 1$  (although we note that a periodicity of 3 is an excellent approximation) and we merely inserted two extra terms of lower periodicity into the potential used for  $\text{CH}_3\text{CH}_2\text{NH}_3^+$ , resulting in the six-parameter function

$$\begin{aligned}
 V(\alpha_1, \alpha_2) = & A_{00}^{cc} + A_{10}^{cc} \cos n_1 \alpha_1 + A_{01}^{cc} \cos n_2 \alpha_2 \\
 & + A_{02}^{cc} \cos 2n_2 \alpha_2 + A_{03}^{cc} \cos 3n_2 \alpha_2 \\
 & + A_{13}^{cc} [\cos n_1 \alpha_1 \cos 3n_2 \alpha_2] \\
 & - |A_{13}^{ss}| [\sin n_1 \alpha_1 \sin 3n_2 \alpha_2]. \quad (17)
 \end{aligned}$$

The potential parameters for all the two-rotor systems we examined are listed in Table X, and were obtained from

analytic fits to  $\text{MP2/6-311+G}(2df,p)$  energies calculated using geometrical structures *completely* optimized at the  $\text{MP2/6-31G}(d)$  level of theory for selected choices of internal torsional angles. Initially the selected points included the conrotated minima and disrotated stationary points for both  $(\text{CH}_3)_2\text{CH}^+$  and  $(\text{CH}_3)_2\text{COH}^+$ , but the fits produced spurious maxima and minima. The selection of ‘‘equidistant’’ points was found to produce better potential functions from both a qualitative and quantitative point of view, including satisfactory conrotated minima and disrotated stationary points. The geometry optimizations were performed by freezing the torsional angle of one of the hydrogen atoms in the rotor, but for fitting purposes the effective rotor torsional angle was taken as the average of the individual hydrogen torsional angles,<sup>54</sup> i.e.,  $\alpha_{\text{eff}} = (\alpha'_1 + \alpha'_2 + \alpha'_3)/3$  for a methyl group, where the  $\alpha'_i$  are given in the range  $180^\circ < \alpha'_i < 180^\circ$ . For example, the optimization of  $(\text{CH}_3)_2\text{CH}^+$  which had one HCCH torsional angle for each methyl group frozen at  $\alpha'_1 = +30^\circ$  resulted in an  $\alpha_{\text{eff}}$  value of  $37.854^\circ$  for each methyl group, because  $\alpha'_2$  and  $\alpha'_3$  became  $164.459^\circ$  and  $-80.896^\circ$  after optimization. Among the convenient aspects of this definition is the satisfaction of the expected symmetries  $V(0^\circ) = V(120^\circ) = V(-120^\circ)$ . The optimized points used for the fits are listed in supplementary material.<sup>97</sup> Most (if not all) of the potentials listed in Table X are the best two-dimensional *ab initio* potentials reported for these systems to date, but further improvement could readily be achieved if required for spectroscopic (rather than thermodynamic) purposes. The best spectroscopically derived potential for these systems is the second acetone potential of Goodman and co-workers<sup>64</sup> ( $A_{10}^{cc} = -2.28$ ,  $A_{11}^{cc} = 0.86$ ,  $A_{11}^{ss} = -0.99 \text{ kJ mol}^{-1}$ ), which is in excellent agreement with ours ( $A_{10}^{cc} = -2.26$ ,  $A_{11}^{ss} = -A_{11}^{cc} = -0.95 \text{ kJ mol}^{-1}$ ).

## IV. RESULTS AND DISCUSSION

### A. Species without internal rotations

Our results for the absolute entropies (298.15 K, 1 atm) of several molecules and protonated cations, in which internal rotations are absent (and for which the three models E1,

TABLE XI. Third law entropies (298.15 K, 1 atm) for molecules without internal rotors ( $\text{J mol}^{-1} \text{K}^{-1}$ ).<sup>a</sup>

	$S(\text{trans})$	$S(\text{rot})$	$S(\text{vib})$	$S(\text{total})$
CO	150.303	47.523	0.003	197.829
N <sub>2</sub>	150.308	41.637	0.001	191.945
NH <sub>3</sub>	144.101	47.938	0.335	192.374
NH <sub>4</sub> <sup>+</sup>	144.818	40.898	0.218	185.934
H <sub>2</sub> O	144.802	44.022	0.028	188.852
CO <sub>2</sub>	155.939	54.974	3.013	213.927
OCS	159.803	66.065	6.280	232.148
HOCS <sup>+</sup>	160.011	84.357	8.002	252.370
HSCO <sup>+</sup>	160.011	88.471	10.310	258.792
CS <sub>2</sub>	162.749	65.408	9.767	237.924
<sup>32</sup> S <sup>12</sup> C <sup>34</sup> S	163.073	71.420	9.856	244.349
HSCS <sup>+</sup>	162.914	93.347	12.983	269.243
C <sub>4</sub> H <sub>5</sub> N	161.194	95.778	14.072	271.045
C <sub>5</sub> H <sub>5</sub> N	163.248	101.137	18.159	282.544
HCN	149.857	49.677	1.779	201.313
HNC	149.857	49.435	5.877	205.169
CH <sub>2</sub> CO	155.365	77.846	7.993	241.204
C <sub>2</sub> H <sub>4</sub>	150.319	66.404	2.414	219.137
C <sub>2</sub> H <sub>5</sub> <sup>+</sup>	150.760	74.145	6.390	231.294
H <sub>2</sub>	117.489	12.651	0.000	130.140
CH <sub>4</sub>	143.350	42.342	0.395	186.087
HBr	163.387	35.148	0.001	198.535

<sup>a</sup>Results are for the most abundant isotopomer, except for <sup>12</sup>C<sup>32</sup>S<sup>34</sup>S.

E2 and E2, to be discussed in Sec. V, are identical), are presented in Table XI. In all cases, the most abundant isotope of each atom is used, except for the additional <sup>32</sup>S<sup>12</sup>C<sup>34</sup>S isotopomer of carbon disulfide. The entropies are separated into their translational, rotational, and vibrational components. Symmetry effects in the rotational entropies are important when considering reaction entropies; for instance, note the significant reduction of the entropy of ammonia when protonated, due to the increase in symmetry from  $C_{3v}$  to  $T_d$ , and the large increase in entropy of OCS when protonated on either end, due to the decrease in symmetry from  $C_{\infty v}$  to  $C_s$  which creates a third rotational mode. The larger vibrational entropy for HNC compared with HCN indicates that hydrogen isocyanide is a floppier molecule than hydrogen cyanide.

Values of the entropy components at various temperatures are displayed for H<sub>2</sub>O, CS<sub>2</sub>, and pyrrole in Table XII, and demonstrate the expected temperature dependences of

TABLE XII. Temperature dependence of components of third law entropies (1 atm) for molecules without internal rotors ( $\text{J mol}^{-1} \text{K}^{-1}$ ).

	Temp (K)	$S(\text{trans})$	$S(\text{rot})$	$S(\text{vib})$	$S(\text{total})$
H <sub>2</sub> O	298.15	144.802	44.022	0.028	188.852
	500	155.549	50.470	0.442	206.460
	600	159.339	52.743	0.856	212.938
CS <sub>2</sub>	298.15	162.749	65.408	9.767	237.924
	500	173.496	69.707	20.246	263.449
	600	177.286	71.223	24.748	273.257
C <sub>4</sub> H <sub>5</sub> N	298.15	161.194	95.778	14.072	271.045
	500	171.941	102.226	45.715	319.882
	600	175.731	104.500	62.694	342.925

$2.5 R \ln T$  for translation,  $1.5 R \ln T$  for rotation of non-linear molecules, and  $R \ln T$  for rotation of linear molecules. The results for vibrations show a similar temperature dependence, although the exact formula is more complex.

The accuracy of the current results for third-law entropies is demonstrated empirically by comparison with literature values for the neutral species in Table XIII. Generally, the literature results have also been computed via statistical mechanics, but using experimental rather than theoretical values for molecular parameters. For the molecules with no internal rotations, the JANAF<sup>2</sup> and NBS<sup>1</sup> tables are in excellent agreement with one another, with discrepancies of less than  $0.15 \text{ J mol}^{-1} \text{K}^{-1}$  except for formaldehyde, ethene, and ammonia. We have selected the JANAF values as the preferred values for comparison since their treatment is often more detailed; for instance, for NH<sub>3</sub> JANAF incorporates anharmonic and rovibrational coupling for the umbrella mode. For formaldehyde and the molecules having internal rotations, we have preferred the values of Chao *et al.*<sup>58</sup> to the other literature values.

Our current theoretical values represent quite reasonable estimates of absolute third-law entropies, being able to duplicate the JANAF and Chao *et al.* values for no-rotor systems to within  $0.5 \text{ J mol}^{-1} \text{K}^{-1}$  for all molecules except OCS. For OCS, the  $0.6 \text{ J mol}^{-1} \text{K}^{-1}$  discrepancy is due to errors in the degenerate bending frequency ( $0.35 \text{ J mol}^{-1} \text{K}^{-1}$ ), the C-S stretching frequency ( $0.20 \text{ J mol}^{-1} \text{K}^{-1}$ ), the moments of inertia ( $0.15 \text{ J mol}^{-1} \text{K}^{-1}$ ), and non-RRHO effects ( $-0.10 \text{ J mol}^{-1} \text{K}^{-1}$ ). Surprisingly, use of the scaled MP2/6-31G(*d*) harmonic bending frequency, rather than the scaled HF frequency, would actually worsen the error for OCS and cause our entropy for CO<sub>2</sub> to be  $1.1 \text{ J mol}^{-1} \text{K}^{-1}$  too high. We note that bending frequencies of cumulenes are known to be somewhat difficult to obtain *ab initio*. The largest discrepancy between the present results and published values in this section is found for the entropy of acetonitrile (CH<sub>3</sub>CN), where our entropy value lies below that of the NBS tables by  $2 \text{ J mol}^{-1} \text{K}^{-1}$ . The use of experimental fundamentals for vibrational entropy increases our value only by  $0.5 \text{ J mol}^{-1} \text{K}^{-1}$ , leaving a puzzlingly large remaining discrepancy. However, when compared with the value from Lange's Handbook,<sup>3</sup> our result is an underestimate of only  $0.54 \text{ J mol}^{-1} \text{K}^{-1}$ . For ketene, the Lange Handbook value is certainly more appropriate than that of the NBS tables due to an apparent omission by the latter of the  $-R \ln 2$  term which accounts for rotational symmetry.

Isotope effects are fortunately quite minor, but warrant some discussion here. The values for third-law entropies in Table XIII and elsewhere in this work correspond to one mole of a single isotopomer. To compute a third-law entropy for a compound with mole fractions  $x_i$  of various isotopomers  $i$ , one should properly compute

$$S = \sum_i x_i S_i - R \sum_i x_i \ln x_i, \quad (18)$$

where the second sum is the entropy of mixing of isoto-

TABLE XIII. Comparison of absolute entropies ( $\text{J mol}^{-1} \text{K}^{-1}$ ) at 298.15 K and 1 atm.

	This work <sup>a</sup>	Chao <i>et al.</i> <sup>b,f</sup>	Lange <sup>c</sup>	NBS <sup>d,f</sup>	JANAF <sup>e,f</sup>	Error <sup>g</sup>
Molecules with no rotors						
CO	197.83		197.90	197.56	197.54(04)	0.29(04)
N <sub>2</sub>	191.95		191.50	191.50	191.50(02)	0.45(02)
NH <sub>3</sub>	192.37		192.34	192.34	192.66(03)	-0.29(03)
H <sub>2</sub> O	188.85		188.72	188.715	188.72(04)	0.13(04)
H <sub>2</sub> S	205.52		205.77	205.68	205.65	-0.13
CO <sub>2</sub>	213.93		213.68	213.63	213.69(12)	0.24(12)
OCS	232.15		231.46	231.46	231.58	0.57
CS <sub>2</sub>	237.92		237.78	237.73	237.87(08)	0.05(08)
CH <sub>3</sub> CN	242.93		243.47	245.01		
Pyrrrole	271.04					
Pyridine	282.54		282.80			
HF	173.79		173.68	173.67	173.67	0.12
HCN	201.31		201.67	201.67	201.72(04)	-0.41(04)
HNC	205.17					
HCl	186.54		186.77	186.80	186.79	-0.25
CS	210.49		210.46	210.45	210.44(04)	0.05(04)
PH <sub>3</sub>	209.98		210.20	210.12	210.13	-0.15
CH <sub>2</sub> S	230.81					
CH <sub>2</sub> CO	241.20		241.79	247.52 <sup>h</sup>		
CH <sub>2</sub> O	218.72	218.76(04)	218.78	218.66	218.84(40)	-0.04(04)
C <sub>2</sub> H <sub>4</sub>	219.14		219.20	219.45	219.22	-0.08
H <sub>2</sub>	130.14		130.59	130.57	130.57(03)	-0.43(03)
C <sub>2</sub> H <sub>3</sub> CN	273.50					
HCOOH	248.75	248.88(05)	248.74			-0.13(05)
CH <sub>4</sub>	185.94		186.27	186.15	186.14(04)	-0.20(04)
HBr	198.54		198.61	198.58	198.59(03)	-0.05(03)
Molecules with rotors						
CH <sub>3</sub> OH	239.94	239.70(09)	239.70	239.70		0.24(09)
CH <sub>3</sub> NH <sub>2</sub>	242.22		242.59	243.30		
CH <sub>3</sub> SH	255.11			255.06		
Toluene	321.53		320.66			
CH <sub>3</sub> OCHO	286.10	285.17(28)	301.25			0.93(28)
CH <sub>3</sub> CH <sub>2</sub> CN	285.97					
CH <sub>3</sub> CHO	264.01	263.84(22)	264.22	250.2		0.17(22)
CH <sub>3</sub> CHCH <sub>2</sub>	266.82		266.60			
(CH <sub>3</sub> ) <sub>2</sub> O	267.58	267.23(28)	267.06	266.27		0.35(28)
(CH <sub>3</sub> ) <sub>2</sub> NH	273.79		272.96	272.96		
(CH <sub>3</sub> ) <sub>2</sub> S	286.33		285.85	285.85		
(CH <sub>3</sub> ) <sub>2</sub> CO	295.92	297.51(45)	294.93			-1.59(45)
CH <sub>3</sub> CH <sub>2</sub> NH <sub>2</sub>	282.94		284.85			
(CH <sub>3</sub> ) <sub>2</sub> CCH <sub>2</sub>	293.37		293.59			
(CH <sub>3</sub> ) <sub>3</sub> N	290.08		288.78	287.0		

<sup>a</sup>Corresponds to the E3 procedure (see Section V).

<sup>b</sup>Chao *et al.* (Ref. 58).

<sup>c</sup>Lange Handbook (Ref. 3).

<sup>d</sup>NBS Tables (Ref. 1).

<sup>e</sup>JANAF Tables (Ref. 2).

<sup>f</sup>These values have been lowered by  $0.11 \text{ J mol}^{-1} \text{K}^{-1}$  from the original 1 bar=0.1 MPa values to correspond to 1 atm=0.101325 MPa values.

<sup>g</sup>Difference between current values and those of JANAF or Chao *et al.*

<sup>h</sup>Erroneously too high by  $R \ln 2$ .

omers. When reaction entropies  $\Delta S$  are computed, the contributions due to mixing and rotational symmetry combine to exactly cancel out all their isotope probability terms, and hence the only effect of isotopes for reaction entropies will be due to mass, vibrational frequencies, and moments of inertia, which will largely cancel as well. Hence we use only the most abundant atomic isotopes in our calculations for third-law entropies. To examine the effect of isotopes on an absolute entropy, we computed entropies for the two most

abundant isotopomers of carbon disulfide,  $^{32}\text{S}^{12}\text{C}^{32}\text{S}$  (denoted CS<sub>2</sub> in Table XI and following tables) and  $^{32}\text{S}^{12}\text{C}^{34}\text{S}$ . From the breakdown in Table XI one can see that the entropies for these two forms differ primarily by the  $-R \ln 2$  symmetry term ( $=5.76 \text{ J mol}^{-1} \text{K}^{-1}$ ), absent for  $^{32}\text{S}^{12}\text{C}^{34}\text{S}$ . The weighted average entropy at 298.15 K is  $0.92 S^\circ(^{32}\text{S}^{12}\text{C}^{32}\text{S}) + 0.08 S^\circ(^{32}\text{S}^{12}\text{C}^{34}\text{S}) = 238.44 \text{ J mol}^{-1} \text{K}^{-1}$ , which becomes  $240.76 \text{ J mol}^{-1} \text{K}^{-1}$  with the entropy of mix-

TABLE XIV. Comparison of methods (298.15 K, 1 atm) for calculation of the entropy of single internal rotations ( $\text{J mol}^{-1} \text{K}^{-1}$ ).

	$S(Q_{\text{HO}})$	$S(Q_{\text{hind}})$	$S(Q_f)$
CH <sub>3</sub> OH	5.666	7.345	8.358
CH <sub>3</sub> OH <sub>2</sub> <sup>+</sup>	8.324	9.133	10.518
CH <sub>3</sub> NH <sub>2</sub>	5.833	7.467	10.742
CH <sub>3</sub> NH <sub>3</sub> <sup>+</sup>	6.737	7.475	11.870
CH <sub>3</sub> SH	7.777	9.107	10.673
CH <sub>3</sub> SH <sub>2</sub> <sup>+</sup>	8.352	9.184	12.330
Toluene	31.643	14.838 <sup>a</sup>	14.838
<i>p</i> -C <sub>7</sub> H <sub>9</sub> <sup>+</sup>	20.560	14.874 <sup>a</sup>	14.874
<i>o</i> -C <sub>7</sub> H <sub>9</sub> <sup>+</sup>	24.599	14.863 <sup>a</sup>	14.863
CH <sub>3</sub> OCHO	11.209	12.987	14.792
CH <sub>3</sub> OCHOH <sup>+</sup>	14.343	14.099	14.864
CH <sub>3</sub> CH <sub>2</sub> CN	8.403	8.646	14.590
CH <sub>3</sub> CH <sub>2</sub> CNH <sup>+</sup>	8.904	9.413	14.626
CH <sub>3</sub> CHO	11.974	12.056	13.495
<i>cis</i> -CH <sub>3</sub> CHOH <sup>+</sup>	13.154	11.052	13.752
<i>trans</i> -CH <sub>3</sub> CHOH <sup>+</sup>	14.198	10.752	13.711
CH <sub>5</sub> <sup>+</sup>	11.897	6.379 <sup>a</sup>	6.379
CH <sub>3</sub> CHCH <sub>2</sub>	9.381	10.254	13.801

<sup>a</sup>Internal rotation barrier is assumed negligible.

ing. The value for one mole of <sup>32</sup>S<sup>12</sup>C<sup>32</sup>C in Table XIII is 237.92  $\text{J mol}^{-1} \text{K}^{-1}$ . In tabulations such as those of NBS<sup>1</sup> and JANAF<sup>2</sup>, the isotope effects which would cancel when computing a reaction entropy (i.e., the rotational symmetry and entropy of mixing terms mentioned above) are ignored, but the other isotope effects are generally included. Hence, the proper comparison in Table XIII with the literature entropies for carbon disulfide is best done with a value obtained by including the  $-R \ln 2$  term into  $S^\circ(^{32}\text{S}^{12}\text{C}^{34}\text{S})$  before performing the isotope averaging; this removes the effect of isotopes upon rotational symmetry and allows one to ignore the entropy of mixing of isotopomers altogether. The  $-R \ln 2$  symmetry term is retained because users of the literature values would assume a rotational symmetry of 2 for CS<sub>2</sub>, and can be proven to arise from proper consideration of the rotational symmetry and entropy of mixing terms. This adjustment before averaging results in an  $S_{298.15}^\circ$  of 237.98  $\text{J mol}^{-1} \text{K}^{-1}$ , which is little different from the <sup>32</sup>S<sup>12</sup>C<sup>32</sup>S value of 237.92, and hence we conclude that isotope effects are quite minor.

## B. Species with one internal rotation

To evaluate the importance of the hindered rotor model on third-law entropies, Table XIV presents the results (298.15 K, 1 atm) for the entropies of various single internal rotations using three different models for the canonical partition function. The hindered rotor entropies were found by linear interpolation of the values in the Pitzer tables, using our data which was presented in Tables V and VII for some of these species. The hindered rotor model with barrier height  $V_0$  can be extrapolated to the free rotor (if  $V_0 \rightarrow 0$ , for which the entropy is

$$S(Q_f) = 1/2R \ln[e \pi / \sigma^2 \theta_{\text{rot}}] + 1/2R \ln T, \quad (19)$$

TABLE XV. Temperature dependence (1 atm) of entropy of single internal rotations ( $\text{J mol}^{-1} \text{K}^{-1}$ ).

	Temp (K)	$S(Q_{\text{HO}})$	$S(Q_{\text{hind}})$	$S(Q_f)$
CH <sub>3</sub> OH	298.15	5.666	7.345	8.358
	500	9.497	10.059	10.508
	600	10.931	10.949	11.266
Toluene	298.15	31.643	14.838 <sup>a</sup>	14.838
	500	35.941	16.987 <sup>a</sup>	16.987
	600	37.456	17.745 <sup>a</sup>	17.745
CH <sub>3</sub> CH <sub>2</sub> CN	298.15	8.403	8.646	14.590
	500	12.471	13.277	16.739
	600	13.948	14.801	17.497
CH <sub>3</sub> CHO	298.15	11.974	12.056	13.495
	500	16.178	15.049	15.644
	600	17.678	15.989	16.402

<sup>a</sup>Internal rotation barrier is assumed negligible.

where  $\sigma$  is the rotor symmetry number,  $R = 8.314511 \text{ J mol}^{-1} \text{K}^{-1}$ ,  $e \approx 2.71828$  is the natural log base, and  $\theta_{\text{rot}}$  is the rotor rotational temperature constant

$$\theta_{\text{rot}} = h^2 / 8\pi^2 I k, \quad (20)$$

where  $h$  is Planck's constant,  $k$  is Boltzmann's constant, and  $I$  is the rotor's reduced moment of inertia. The hindered rotor model also can be extrapolated (if  $V_0 \rightarrow +\infty$  and  $T$  small) to the harmonic oscillator, for which the entropy is

$$S(Q_{\text{HO}}) = R(\theta_{\text{vib}}/T)(e^{\theta_{\text{vib}}/T} - 1)^{-1} - R \ln[1 - e^{-\theta_{\text{vib}}/T}], \quad (21)$$

where  $\theta_{\text{vib}}$  is the torsional vibrational temperature constant

$$\theta_{\text{vib}} = h\omega/k \quad (22)$$

and we take the harmonic oscillator frequency  $\omega$  to be the scaled HF/6-31G(*d*) torsional harmonic frequency. The HF/6-31G(*d*) scaled harmonics are not expected to reproduce the true torsional fundamentals, nor the harmonics obtainable from the cosine potential, but are used to examine the performance of the harmonic oscillator approximation for torsional modes with low barriers.

Table XV examines the temperature dependence of these three models of internal rotation entropy for four selected molecules. The high temperature asymptotic limit of the entropy from a harmonic oscillator is  $R - R \ln \theta_{\text{vib}} + R \ln T$ , which reveals a temperature dependence which is double that appropriate for an internal rotation. In Tables XIV and XV, however, the temperatures are not sufficiently high for that incorrect high-temperature asymptote to be a problem, except for the modes with very low torsional harmonic frequencies which consequently produce very high estimates of entropies (e.g., toluene and, later, acetone). In fact, one can see in Table XV when going from 298 K to 600 K that the harmonic oscillator entropies are indeed rising relative to the free rotor results.

For the internal rotations in Table XIV, the  $S(Q_{\text{hind}})$  values at 298 K are generally larger than those of the harmonic oscillators, and always lower than the free rotor  $S(Q_f)$  val-

TABLE XVI. Third law entropies (298.15 K, 1 atm) for molecules with internal rotors ( $\text{J mol}^{-1} \text{K}^{-1}$ ).<sup>a</sup>

	$S(\text{trans})$	$S(\text{rot})$	$S(\text{vib})$	$S(\text{hind})$	$S(\text{total})$
$\text{CH}_3\text{OH}$	151.981	79.507	1.109	7.345	239.943
Toluene	165.150	107.134	34.408	14.838	321.530
$\text{CH}_3\text{CH}_2\text{CN}$	158.735	100.004	18.586	8.646	285.972
$\text{CH}_3\text{CHO}$	155.950	90.646	5.356	12.056	264.007
$\text{CH}_5^+$	144.110	60.738	0.931	6.379	212.158
$(\text{CH}_3)_2\text{O}$	156.508	86.528	5.911	18.630	267.577
$(\text{CH}_3)_2\text{CO}$	159.397	95.304	13.854	27.367	295.921
$\text{CH}_3\text{CH}_2\text{NH}_2$	156.238	93.980	8.324	24.399	282.942
$(\text{CH}_3)_3\text{C}^+$	159.186	87.411	18.527	44.449	309.572

<sup>a</sup>The division of symmetry number effects into  $S(\text{rot})$  and  $S(\text{hind})$  is somewhat arbitrary. For cases where we assumed free rotors (toluene,  $(\text{CH}_3)_3\text{C}^+$ ,  $\text{CH}_5^+$ ), we chose  $\sigma_{\text{int}}=3$  consistently. For  $\text{CH}_3\text{CH}_2\text{NH}_2$ , the  $S(\text{hind})$  results required use of  $\sigma(\text{NH}_2)=3$  for the Pitzer tables and a further  $R \ln 3$  added to remove the false symmetry effect.

ues. The first of these observations indicates not only that the high-temperature limits are not approached, but also that the anharmonicity of the torsional potential surface in the  $Q_{\text{hind}}$  model is causing the energy levels to be more congested than predicted by a harmonic potential. The exceptions ( $\text{CH}_5^+$ ,  $\text{CH}_3\text{CHOH}^+$ , and  $\text{CH}_3\text{OCHOH}^+$  in Table XIV) occur with small barrier systems, where the torsional frequency is sufficiently small that the crossover by  $S(Q_{\text{HO}})$  caused by the incorrect high- $T$  limit occurs at quite a low temperature. As a function of barrier height, the crossover occurs at roughly 3–5  $\text{kJ mol}^{-1}$  at 298 K, the precise value depending on the moment of inertia. For barriers of this magnitude or lower, the free rotor  $S(Q_f)$  value becomes accurate to within  $\sim 2 \text{ J mol}^{-1} \text{K}^{-1}$ . This suggests that a procedure which uses  $S(Q_{\text{HO}})$  for systems with barriers  $>3.5 \text{ kJ mol}^{-1}$  and  $S(Q_f)$  for barriers  $<3.5 \text{ kJ mol}^{-1}$  to calculate entropies at 298 K can achieve  $\sim 2 \text{ J mol}^{-1} \text{K}^{-1}$  accuracy, which leads to the E1 model of Section V.

Our best calculated total entropies for species with just one internal rotation mode (298.15 K, 1 atm) are presented in the top part of Table XVI. The entries for the internal rotation are labelled  $S(\text{hind})$  whether treated as hindered or free rotations. Note that the systems with four or more first-row atoms have enough low-frequency vibrations to cause  $S(\text{vib})$  to climb above  $10 \text{ J mol}^{-1} \text{K}^{-1}$ , suggesting that the specialized scaling of “heavy-atom” bending mode frequencies (rather than the traditional use of general scale factors for all frequencies) could be a source of improvement in accuracy for molecules of this size.

For comparisons of these statistical entropies with literature values we return to Table XIII. Agreement is generally found to within  $0.5 \text{ J mol}^{-1} \text{K}^{-1}$  of the best literature results, although two cases warrant attention. For  $\text{CH}_3\text{NH}_2$ , our  $S^{298.15}$  value is below that of the NBS tables<sup>1</sup> by  $1.1 \text{ J mol}^{-1} \text{K}^{-1}$ . The use of experimental fundamentals for vibrational entropy worsens the discrepancy to  $1.2 \text{ J mol}^{-1} \text{K}^{-1}$  but, as with  $\text{CH}_3\text{CN}$ , our result for  $\text{CH}_3\text{NH}_2$  compares more favorably with the Lange Handbook<sup>3</sup> value which lies only  $0.4 \text{ J mol}^{-1} \text{K}^{-1}$  higher. Coupling of the internal rotation with the  $\text{NH}_2$  inversion mode, which has prob-

ably not been considered to date, may be significant. For  $\text{CH}_3\text{OCHO}$ , our  $S^{298.15}$  value is above that of Chao *et al.*<sup>58</sup> by  $0.9 \text{ J mol}^{-1} \text{K}^{-1}$ . Use of experimental fundamentals reduces our value by  $1.1 \text{ J mol}^{-1} \text{K}^{-1}$ , accounting for the discrepancy. Our value has a large error in this case arising from relatively small errors in the calculated low frequency vibrations corresponding to the COC bend and  $\text{CH}_3\text{O}-\text{CHO}$  torsion. Although both are underestimated by only  $20 \text{ cm}^{-1}$ , this effect is greatly magnified because the absolute magnitudes of the fundamentals are so low ( $\sim 300 \text{ cm}^{-1}$ ). This example highlights the sensitivity of the calculated entropies to the low frequency vibrations.

### C. Species with two internal rotations

For the species with two internal rotation modes, nine separate estimates of the contribution to the third-law entropy from these two modes were computed, and these are listed in Table XVII with labels A to I. Many approximations were examined, primarily in an effort to find a suitably accurate independent-mode approximation that might allow us to avoid a two-dimensional numerical integration and perhaps the use of  $Q_{\text{Scaled}}$  as well. Our best estimates are shown in the rightmost Column I, and arise from use of  $Q_{\text{Scaled}}$ , with the two-dimensional potential energy surfaces (PESs) described in Section III C used in  $Q_{\text{Class}}$ , and their normal mode frequencies (see for example Equation 15) used in  $Q_{\text{HO Quant}}$  and  $Q_{\text{HO Class}}$ . These are of use in assessing the results of more approximate models.

The three varieties of independent-mode hindered-rotor approximations (ind.) which we examined, designated “low,” “medium,” and “high”, are also independent-rotor approximations, in contrast to the all-HO model, whose independent  $a_2$  and  $b_1$  torsional modes ( $C_{2v}$  molecules) each involve a coupling of the two methyl rotations. The low-medium-high designations refer to the modification of the three parameters of the uncoupled potential ( $A_{00}$ ,  $A_{10}$ , and  $A_{01}$ ) to produce single rotor barriers of  $V(0,60) - V(0,0)$ ,  $0.5*[V(60,60) - V(0,0)]$ , and  $V(60,60) - V(60,0)$ , respectively, except in the model described by column B (our Pitzer table method) for which the single-rotor barriers correspond to the energy differences between the global minima and single rotor maxima. In the usual case of  $A_{11}^{cc} > 0$ ,  $V(0,60) - V(0,0)$  has a lower value than  $V(60,60) - V(60,0)$ . Hence, use of the “low” barrier (columns B, E, and H in Table XVII) should give an upper-bound entropy in the  $A_{11}^{cc} > 0$  cases (and lower-bound entropy in the  $A_{11}^{cc} < 0$  cases), while use of the “high” barrier (not shown) should give a lower-bound entropy in the  $A_{11}^{cc} > 0$  cases (upper bound for  $A_{11}^{cc} < 0$ ).

Use of the “medium” barrier tended to give entropies which were too low, because at our temperatures the  $V(0,0)$ -to- $V(0,60)$  regions of the potential surfaces of these molecules are “sampled” more often than the  $V(0,60)$ -to- $V(60,60)$  regions. However, knowing *a priori* whether the “low” or “medium” barrier will provide the better estimate of third-law entropy at a given temperature appears difficult. Certainly the higher  $V(0,60)$  is, the better the “low” barrier

estimator becomes [e.g., see  $(\text{CH}_3)_2\text{NH}$  and  $(\text{CH}_3)_2\text{NH}_2^+$ , which have large single-rotor barriers].

The differences between columns B and H are due only to the use of the  $Q_{\text{Scaled}}$  approximation, except for  $(\text{CH}_3)_2\text{CH}^+$  and  $(\text{CH}_3)_2\text{COH}^+$  for which (i)  $A_{20}$  and  $A_{02}$  terms are present in the full potential and are retained for all  $Q_{\text{Scaled}}$  results, and (ii) the single-rotor barrier heights used for calculation of column B results are obtained as energy differences between global minima and single-rotor maxima. Hence the differences between columns B and H for the ten other species should be just double those of our earlier single-rotor test table, Table VIII. At 600 K the differences between  $S(Q_{\text{Scaled}})$  and  $S(Q_{\text{Hind}})$  are generally  $+0.02$  to  $+0.06 \text{ J mol}^{-1} \text{ K}^{-1}$  which is consistent with our test table results for  $V/RT$  values of 4 or less. Columns D–F differ from columns G–I by using the scaled HF/6-31G(d) harmonic frequencies in  $Q_{\text{HO Quant}}$  and  $Q_{\text{HO Class}}$ , rather than the normal mode frequencies computed from the MP2/6-311+G(2df,p) PESs. The differences between the results in columns D–F and their counterparts in columns G–I are small, generally  $0.3 \text{ J mol}^{-1} \text{ K}^{-1}$  at 298 K and less than  $0.1 \text{ J mol}^{-1} \text{ K}^{-1}$  at 600 K, and positive, suggesting that the scaled HF/6-31G(d) harmonic frequencies for internal rotation modes have a consistent remaining error, relative to the MP2/6-311+G(2df,p) values.

The special case of an internal rotation between two non-cylindrically symmetric groups was encountered only once in our molecule set, that being the rotation of the amino group against the ethyl group in ethylamine. Four energetically distinct stationary points are present, a *trans* minimum (where the nitrogen lone pair is *trans* to the methyl group), a *cis* maximum, a pair of energetically equivalent  $C_1$ -symmetry *gauche* minima, and a similar pair of  $C_1$ -symmetry maxima. The MP2/6-311+G(2df,p) relative energies of the MP2/6-31G(d) optimized conformations (in  $\text{kJ mol}^{-1}$ ) are: *gauche* minimum 0.0, *trans* minimum 0.7,  $C_1$ -symmetry maximum 9.9, *cis* maximum 8.2. The various barrier heights were averaged in order to use the simple potential form in Equation (3) and hence the Pitzer tables (column B of Table XVII). At MP2/6-31G(d), the *trans* conformer is actually the lowest in energy, and hence our HF frequencies and MP2 rotor moments of inertia were computed for the *trans* conformer. On the other hand, the results in Tables XVI and XVII for  $\text{CH}_3\text{CH}_2\text{NH}_2$  using  $Q_{\text{Scaled}}$  employ PES normal mode frequencies computed at its *gauche* minimum; the two-dimensional results change less than  $0.01 \text{ J mol}^{-1} \text{ K}^{-1}$  if the *trans*-conformer PES frequencies are used.

The asymmetric rotation about the C–N bond in ethylamine is also the only case encountered in this study in which one cannot simply use the torsional periodicity  $n$  of Eq. (3) as the internal rotation symmetry number  $\sigma$  in the partition function. With the free rotor model,  $\sigma$  should be taken as 1 because all rotor positions are distinguishable (even the two *gauche* forms are enantiomers). Alternatively, one could use  $\sigma=3$  in the formula but add  $R \ln 3$  to account for this distinguishability. With the harmonic oscillator model, one considers the three minima as corresponding to

distinct isomers, and hence an entropy of mixing of the three is added, approximated by  $R \ln 3$  and included in Tables XVI and XVII. The hindered rotor result is also obtained by using  $\sigma=3$  in its formula for the Pitzer tables, but adding  $R \ln 3$  to account for distinguishability; this is equivalent to using the free rotor model with  $\sigma=1$  but adding corrections for a potential of periodicity 3. Hence the extra  $R \ln 3$  can be shown to appear in all three treatments of the asymmetric Et-NH<sub>2</sub> torsion mode of ethylamine.

For dimethyl systems, the harmonic oscillator approximation (column A of Table XVII) produces errors (compared with our best results shown in column I) in third-law entropy which vary from  $-1.7 \text{ J mol}^{-1} \text{ K}^{-1}$  (for  $(\text{CH}_3)_2\text{O}$  and  $(\text{CH}_3)_2\text{S}$ ) to greater than  $+6 \text{ J mol}^{-1} \text{ K}^{-1}$  (for  $(\text{CH}_3)_2\text{CO}$ ) at 298 K. The free rotor approximation (column C) generally produces larger errors, up to  $+12 \text{ J mol}^{-1} \text{ K}^{-1}$  at 298 K (for  $(\text{CH}_3)_2\text{NH}$ ), although it comes within  $1 \text{ J mol}^{-1} \text{ K}^{-1}$  of our best results for  $(\text{CH}_3)_2\text{CO}$  and  $(\text{CH}_3)_2\text{COH}^+$  at the higher temperatures, in which cases the model becomes more appropriate. The Pitzer-table method (column B) shows a maximum error of  $-1.4 \text{ J mol}^{-1} \text{ K}^{-1}$  (for  $(\text{CH}_3)_2\text{CH}^+$ , which is least well suited by single cosine potentials). The independent-mode method with the lowest maximum deviation [ $-1.1 \text{ J mol}^{-1} \text{ K}^{-1}$  for  $(\text{CH}_3)_2\text{O}$ ] relative to our best results is the column G method, which can incorporate more complex one-dimensional potentials.

The other components of the third-law entropies of species with two internal rotation modes are computed as before, and are displayed for  $(\text{CH}_3)_2\text{O}$ ,  $(\text{CH}_3)_2\text{CO}$ , and  $\text{CH}_3\text{CH}_2\text{NH}_2$  in Table XVI.

For comparisons of our best values with literature values, we return to Table XIII. For these multirotor systems, our values are probably as good (if not better) than previous literature values derived from experimental data, and deviations of  $1 \text{ J mol}^{-1} \text{ K}^{-1}$  are not dissatisfying. The  $-1.59 \text{ J mol}^{-1} \text{ K}^{-1}$  discrepancy between our value for acetone and that of Chao *et al.*<sup>58</sup> suggests an error in the latter; Chao has an earlier value<sup>98</sup> ( $295.3 \text{ J mol}^{-1} \text{ K}^{-1}$ ) which is similarly computed, and while we can reproduce his earlier value (with the Pitzer tables instead of his summation technique) to within  $0.2 \text{ J mol}^{-1} \text{ K}^{-1}$  we cannot do so for his later value, arriving at a value within  $0.3 \text{ J mol}^{-1} \text{ K}^{-1}$  of his older one. In addition, if our barrier heights for acetone were raised from 2.6 to 3.3  $\text{kJ mol}^{-1}$ , to mimic what Chao *et al.* may have used, our third-law entropy would actually be *reduced*, increasing the  $-1.59 \text{ J mol}^{-1} \text{ K}^{-1}$  discrepancy.

#### D. Species with three internal rotations

A full analysis of three-dimensional coupling was deemed beyond the scope of the present work. We examined three triple-rotor species, but only with HO or free-rotor approximations. The internal rotation barrier heights for a single methyl rotation in  $(\text{CH}_3)_3\text{N}$  and  $(\text{CH}_3)_3\text{NH}^+$  in Table V are 18.52 and 14.24  $\text{kJ mol}^{-1}$ , respectively, which are sufficiently high for the harmonic oscillator approximation to be

satisfactory (leading to entropies which are perhaps up to  $2 \text{ J mol}^{-1} \text{ K}^{-1}$  too low for the total entropy of  $(\text{CH}_3)_3\text{NH}^+$  with a smaller error for  $(\text{CH}_3)_3\text{N}$ ).

The tertiary-butyl cation,  $(\text{CH}_3)_3\text{C}^+$ , has a somewhat more interesting potential surface associated with the facile internal rotations of the three methyl groups. On the one hand, two of the three MP2/6-31G(*d*) normal mode frequencies corresponding to internal rotation in  $(\text{CH}_3)_3\text{C}^+$  are almost of the same magnitude as those in isobutene, for which use of the free rotor model would lead to overestimation of the contribution to the total entropy by almost  $9 \text{ J mol}^{-1} \text{ K}^{-1}$ . On the other hand, the entire torsional potential surface of  $(\text{CH}_3)_3\text{C}^+$  (three torsional dimensions) fits within an approximately  $6 \text{ kJ mol}^{-1}$  span, which is much flatter than in isobutene where the two-dimensional surface spans about  $21 \text{ kJ mol}^{-1}$  (with a single-rotor barrier height of about  $9 \text{ kJ mol}^{-1}$ ), which suggests that the free rotor model should do much better for the tertiary-butyl cation than for isobutene. The combination of these two factors may mean that the free rotor approximation performs well for  $(\text{CH}_3)_3\text{C}^+$  at higher temperatures (e.g., 500–600 K) while at lower temperatures the complex three-dimensional hindrances become increasingly important and affect the applicability of the free rotor model to an unknown extent. In this case, it is possible that a three-dimensional potential surface function of accuracy comparable to that of the two-dimensional *ab initio* surfaces used in the previous section could significantly improve the current, free-rotor-based 298 K result.

## V. THEORETICAL MODELS FOR COMPUTING ENTROPIES

We now define three different procedures for computing *ab initio* third-law entropies in general. The simplest of these procedures, designated E1, uses MP2/6-31G(*d*) structures for the rotational entropy and HF/6-31G(*d*) frequencies scaled by 0.8929 with the harmonic oscillator approximation for all internal modes, except for internal rotations having very small barriers, which are treated as free rotations. Here a “very small barrier” is defined as less than  $1.4 RT$  at the MP2/6-31G(*d*) level of theory, which corresponds to  $3.5 \text{ kJ mol}^{-1}$  at 298 K and  $7.0 \text{ kJ mol}^{-1}$  at 600 K. As a compromise between accuracy and efficiency, the moment of inertia approximation for the (relatively rare) free-rotor substitutions in the E1 model is taken as  $I^{(2,1)}$ .

The next procedure, designated E2, is identical to E1 except for the treatment of all internal rotation modes, for which independent-mode internal rotation barrier heights are computed at the MP2/6-311+G(2*df*,*p*)/MP2/6-31G(*d*) level of theory, the  $I^{(m,n)}$  approximations  $I^{(3,1)}$ ,  $I^{(4,1)}$ ,  $I^{(3,4)}$ , and  $I^{(4,4)}$  are calculated (for symmetric single rotor, symmetric multi-rotor, asymmetric single rotor, and asymmetric multi-rotor systems respectively), and the Pitzer tables used to provide their entropy contributions. This procedure could conceivably be automated if the Pitzer tables are installed as a computer database file and a computer program written to compute the internal rotor moments of inertia. Alternatively, as a modification to E2, a functional form could be devel-

oped to reproduce the numerical results of the Pitzer tables to a somewhat lowered accuracy, which has been done previously.<sup>99,100</sup>

The method of highest accuracy presented in this paper we designate as a third-level or E3 procedure, which is identical to the E2 procedure except for systems with two internal rotations. In these cases, E3 requires additional MP2/6-31G(*d*) geometry optimizations, and MP2/6-311+G(2*df*,*p*) energy points are used to analytically fit a coupled potential energy function, which is used in an approximate, scaled partition function ( $Q_{\text{Scaled}}$ ) together with numerical two-dimensional integration to produce the entropy for the internal rotation modes. Establishing a general recipe for constructing the internal rotation potential surfaces which is appropriate for all multirotor cases will require future research, and may not result in an attractive method, particularly if triple-rotor cases like  $(\text{CH}_3)_2\text{NOH}$  or rotor-in-rotor cases like diethylether will require much more *ab initio* data. The E1, E2 and E3 models for systems with two internal rotations correspond to the entries in columns A, B and I, respectively, of Table XVII, except that E1 values for acetone and protonated acetone would employ the free rotor approximation.

Table XVIII compares the results (298.15 K, 1 atm) of the E1, E2, and E3 procedures for the molecules listed in Table XIII, minus the non-rotor molecules for which no JANAF<sup>2</sup> or Chao *et al.*<sup>58</sup> values are available. Mean absolute and maximum deviations (relative to literature values or to E3 values) are listed in the table, although the sample sizes for the molecules involving one and two internal rotations are so small that the statistics are suggestive, rather than truly indicative.

For the molecules without internal rotations, all three methods are identical, and for the test set of 19 molecules the calculated entropies show a mean absolute deviation of  $0.21 \text{ J mol}^{-1} \text{ K}^{-1}$  and a maximum deviation of  $+0.57 \text{ J mol}^{-1} \text{ K}^{-1}$  relative to the chosen literature values. A simpler version of the E1 procedure which avoids the MP2 optimization is to use the HF/6-31G(*d*) structures for the rotational entropies. With this simplification, the mean absolute deviation and maximum deviation for this test set approximately double to 0.4 and  $-1.0 \text{ J mol}^{-1} \text{ K}^{-1}$ , respectively.

For the molecules with single rotors, the E1 values deviate from E2 (or E3) values by  $-0.9$  to  $-1.8 \text{ J mol}^{-1} \text{ K}^{-1}$ , except for ethyl cyanide, acetaldehyde, and toluene ( $-0.2$ ,  $-0.1$ , and  $0.0 \text{ J mol}^{-1} \text{ K}^{-1}$  respectively). The E1 result for ethyl cyanide is good because the high barrier to internal rotation ( $13.4 \text{ kJ mol}^{-1}$ ) makes the HO approximation a good one. The E1 result for acetaldehyde (barrier= $4.7 \text{ kJ mol}^{-1}$ ) is fortuitously good because of the early onset of the incorrect high-*T* asymptote of the harmonic oscillator, which can be seen in the results of Table XV and was noted earlier for  $\text{CH}_3\text{CHOH}^+$ . Toluene represents the extreme case of this incorrect high-*T* asymptote. Use of the harmonic oscillator approximation leads to an error of  $+22.6 \text{ J mol}^{-1} \text{ K}^{-1}$ . This is the motivation for treating low frequency torsions, which will frequently be associated with sixfold or approximately sixfold symmetries, as free rotors

TABLE XVII. Comparison of methods for the calculation of entropy of multiple internal rotations (298.15 K, 500 K, 600 K; 1 atm; J mol<sup>-1</sup> K<sup>-1</sup>).

Column label	A	B	C	D	E	F	G	H	I
Partition function <sup>a</sup>	$Q_{\text{HO}}$	$Q_{\text{hind}}$	$Q_f$	$Q_{\text{scaled}}$	$Q_{\text{scaled}}$	$Q_{\text{scaled}}$	$Q_{\text{scaled}}$	$Q_{\text{scaled}}$	$Q_{\text{scaled}}$
Frequency used in $Q_{\text{HO}}$ <sup>b</sup>	HF			HF	HF	HF	PES	PES	PES
Potential used <sup>c</sup>	HF	Low ind.	0	Med. ind.	Low ind.	Full	Med. ind.	Low ind.	Full
298.15 K									
(CH <sub>3</sub> ) <sub>2</sub> CH <sup>+</sup>	23.620	22.782	27.861	23.138	25.902	23.470	23.549	26.192	24.174
(CH <sub>3</sub> ) <sub>2</sub> O	16.897	18.365	28.266	19.251	18.210	18.500	19.319	18.353	18.630
(CH <sub>3</sub> ) <sub>2</sub> OH <sup>+</sup>	22.092	22.939	28.587	22.129	22.816	22.536	22.323	22.968	22.681
(CH <sub>3</sub> ) <sub>2</sub> NH	15.330	16.420	28.423	16.620	16.203	16.292	16.740	16.358	16.443
(CH <sub>3</sub> ) <sub>2</sub> NH <sub>2</sub> <sup>+</sup>	16.843	18.068	28.725	16.307	17.910	17.540	16.564	18.037	17.651
(CH <sub>3</sub> ) <sub>2</sub> S	19.728	21.500	29.307	21.293	21.366	21.342	21.417	21.486	21.461
(CH <sub>3</sub> ) <sub>2</sub> SH <sup>+</sup>	20.470	21.575	29.421	20.209	21.406	21.024	20.433	21.559	21.173
(CH <sub>3</sub> ) <sub>2</sub> CO	33.439	28.529	29.545	26.707	28.593	27.341	26.866	28.624	27.367
(CH <sub>3</sub> ) <sub>2</sub> COH <sup>+</sup>	29.639	28.930	29.574	27.512	29.351	28.029	27.551	29.281	28.061
CH <sub>3</sub> CH <sub>2</sub> NH <sub>2</sub>	23.033 <sup>d</sup>	24.323	34.564	24.144	24.163	24.158	24.383	24.400	24.399
CH <sub>3</sub> CH <sub>2</sub> NH <sub>3</sub> <sup>+</sup>	15.812	17.140	28.215	15.989	16.961	16.746	16.214	17.101	16.877
(CH <sub>3</sub> ) <sub>2</sub> CCH <sub>2</sub>	19.705	21.399	29.508	19.774	21.269	20.809	19.973	21.379	20.916
500 K									
(CH <sub>3</sub> ) <sub>2</sub> CH <sup>+</sup>	32.020	29.917	32.160	29.786	31.279	29.920	29.937	31.385	30.180
(CH <sub>3</sub> ) <sub>2</sub> O	25.030	27.267	32.564	28.000	27.256	27.601	28.025	27.309	27.649
(CH <sub>3</sub> ) <sub>2</sub> OH <sup>+</sup>	30.440	30.338	32.885	29.985	30.356	30.135	30.055	30.411	30.188
(CH <sub>3</sub> ) <sub>2</sub> NH	23.365	25.650	32.722	25.952	25.590	25.726	25.997	25.648	25.782
(CH <sub>3</sub> ) <sub>2</sub> NH <sub>2</sub> <sup>+</sup>	24.962	27.147	33.024	25.785	27.126	26.594	25.880	27.173	26.635
(CH <sub>3</sub> ) <sub>2</sub> S	28.006	29.801	33.605	29.763	29.809	29.785	29.809	29.853	29.829
(CH <sub>3</sub> ) <sub>2</sub> SH <sup>+</sup>	28.774	29.892	33.720	29.106	29.887	29.494	29.188	29.943	29.548
(CH <sub>3</sub> ) <sub>2</sub> CO	41.942	33.475	33.844	32.734	33.493	32.870	32.791	33.503	32.879
(CH <sub>3</sub> ) <sub>2</sub> COH <sup>+</sup>	38.135	33.629	33.873	33.048	33.787	33.153	33.062	33.762	33.165
CH <sub>3</sub> CH <sub>2</sub> NH <sub>2</sub>	30.953 <sup>d</sup>	32.911	38.863	32.842	32.857	32.851	32.934	32.948	32.943
CH <sub>3</sub> CH <sub>2</sub> NH <sub>3</sub> <sup>+</sup>	23.878	26.184	32.514	25.338	26.152	25.837	25.422	26.205	25.885
(CH <sub>3</sub> ) <sub>2</sub> CCH <sub>2</sub>	27.975	29.808	33.807	28.811	29.819	29.326	28.884	29.859	29.365
600 K									
(CH <sub>3</sub> ) <sub>2</sub> CH <sup>+</sup>	35.018	32.032	33.676	31.892	33.031	31.963	31.997	33.105	32.145
(CH <sub>3</sub> ) <sub>2</sub> O	27.982	30.058	34.080	30.671	30.072	30.391	30.689	30.109	30.424
(CH <sub>3</sub> ) <sub>2</sub> OH <sup>+</sup>	33.429	32.551	34.401	32.295	32.574	32.391	32.344	32.612	32.428
(CH <sub>3</sub> ) <sub>2</sub> NH	26.299	28.708	34.237	29.004	28.693	28.831	29.035	28.734	28.870
(CH <sub>3</sub> ) <sub>2</sub> NH <sub>2</sub> <sup>+</sup>	27.911	30.039	34.539	28.911	30.046	29.521	28.978	30.078	29.549
(CH <sub>3</sub> ) <sub>2</sub> S	30.984	32.292	35.121	32.289	32.325	32.304	32.321	32.355	32.334
(CH <sub>3</sub> ) <sub>2</sub> SH <sup>+</sup>	31.756	32.389	35.236	31.798	32.412	32.063	31.855	32.451	32.101
(CH <sub>3</sub> ) <sub>2</sub> CO	44.958	35.095	35.360	34.576	35.114	34.648	34.615	35.122	34.654
(CH <sub>3</sub> ) <sub>2</sub> COH <sup>+</sup>	41.149	35.221	35.389	34.802	35.328	34.855	34.812	35.311	34.863
CH <sub>3</sub> CH <sub>2</sub> NH <sub>2</sub>	33.867 <sup>d</sup>	35.720	40.379	35.696	35.709	35.703	35.760	35.772	35.767
CH <sub>3</sub> CH <sub>2</sub> NH <sub>3</sub> <sup>+</sup>	26.818	29.125	34.030	28.431	29.124	28.808	28.489	29.160	28.842
(CH <sub>3</sub> ) <sub>2</sub> CCH <sub>2</sub>	30.951	32.345	35.323	31.577	32.377	31.933	31.628	32.405	31.960

<sup>a</sup>Partition function used: HO=harmonic oscillator, hind=rotor hindered by a cosine potential,  $f$ =free rotor, scaled=Pitzer-Gwinn scaled approximation from Eq. (9).

<sup>b</sup>Frequencies used in  $Q_{\text{HO}}$  partition functions (both  $Q_{\text{HO Quant}}$  and  $Q_{\text{HO Class}}$ ): HF=scaled HF/6-31G( $d$ ) torsional harmonics, PES=harmonics from model potentials.

<sup>c</sup>Potential function used in partition function (just in  $Q_{\text{Class}}$  in the case of  $Q_{\text{Scaled}}$ ). "Low ind." refers to independent rotors with lower-bound barrier heights, whereas "med. ind." uses medium barrier heights; see the text.

<sup>d</sup> $R \ln 3$  has been added for asymmetry (entropy of mixing).

within the E1 model. The difference between the E1 and E2 (or E3) values for toluene, due only to the different  $I^{(m,n)}$  approximations, is imperceptible.

For the molecules with two internal rotations, the E1 values deviate from E3 values by  $-1.1$  to  $-1.8$  J mol<sup>-1</sup> K<sup>-1</sup>, except for acetone ( $+2.2$  J mol<sup>-1</sup> K<sup>-1</sup>), for which two free rotors were employed in place of two harmonic oscillators. The barriers to internal rotation in acetone are small enough that the incorrect high- $T$  asymptote makes the harmonic oscillator model a poor approximation (resulting in a  $+6.1$  J mol<sup>-1</sup> K<sup>-1</sup> deviation from E3), hence the replacement by

free rotors in the E1 procedure. The E2 values suggest that E2 does come close to the goal of 1 J mol<sup>-1</sup> K<sup>-1</sup> accuracy, which appears to be the limit for an independent-mode procedure.

## VI. CONCLUSIONS

Three general models for computing third-law entropies for gas-phase molecules or ions have been developed and presented in this study, and are designated E1, E2, and E3. For small, rigid molecules, the three models employ the

TABLE XVIII. Third-law entropies ( $\text{J mol}^{-1} \text{K}^{-1}$ ) derived using the E1, E2 and E3 procedures, at 298.15 K and 1 atm pressure.

Molecules with no rotors			Molecules with one rotor				Molecules with two rotors				
	E1,E2,E3	Literature <sup>a,c</sup>		E1	E2,E3	Literature <sup>b,c</sup>		E1	E2	E3	Literature <sup>b,c</sup>
CO	197.83	197.54(04)	CH <sub>3</sub> OH	238.26	239.94	239.70(09)	(CH <sub>3</sub> ) <sub>2</sub> O	265.84	267.31	267.58	267.23(28)
N <sub>2</sub>	191.95	191.50(02)	CH <sub>3</sub> NH <sub>2</sub>	240.59	242.22		(CH <sub>3</sub> ) <sub>2</sub> NH	272.68	273.77	273.79	
NH <sub>3</sub>	192.37	192.66(03)	CH <sub>3</sub> SH	253.78	255.11		(CH <sub>3</sub> ) <sub>2</sub> S	284.60	286.37	286.33	
H <sub>2</sub> O	188.85	188.72(04)	Toluene	321.53 <sup>d</sup>	321.53		(CH <sub>3</sub> ) <sub>2</sub> CO	298.11 <sup>e</sup>	297.08	295.92	297.51(45)
H <sub>2</sub> S	205.52	205.65	CH <sub>3</sub> OCHO	284.32	286.10	285.17(28)	CH <sub>3</sub> CH <sub>2</sub> NH <sub>2</sub>	281.57 <sup>f</sup>	282.86	282.94	
CO <sub>2</sub>	213.93	213.69(12)	CH <sub>3</sub> CH <sub>2</sub> CN	285.72	285.97		(CH <sub>3</sub> ) <sub>2</sub> CCH <sub>2</sub>	292.16	293.85	293.37	
OCS	232.15	231.58	CH <sub>3</sub> CHO	263.92	264.01	263.84(22)					
CS <sub>2</sub>	237.92	237.87(08)	CH <sub>3</sub> CHCH <sub>2</sub>	265.95	266.82						
HF	173.79	173.67									
HCN	201.31	201.72(04)									
HCl	186.54	186.79									
CS	210.49	210.44(04)									
PH <sub>3</sub>	209.98	210.13									
CH <sub>2</sub> O	218.72	218.76(04) <sup>b</sup>									
C <sub>2</sub> H <sub>4</sub>	219.14	219.22									
H <sub>2</sub>	130.14	130.57(03)									
HCOOH	248.75	248.88(05)									
CH <sub>4</sub>	185.94	186.14(04)									
HBr	198.54	198.59(03)									
Dev  <sup>g</sup>	0.21			1.0	...			1.6	0.34	...	
Max dev <sup>g</sup>	+0.57			+1.8	...			+2.2	+1.16	...	

<sup>a</sup>JANAF Tables (Ref. 2), except where indicated.

<sup>b</sup>Chao *et al.* (Ref. 58).

<sup>c</sup>These values have been lowered by  $0.11 \text{ J mol}^{-1} \text{K}^{-1}$  from the original 1 bar=0.1 MPa values to correspond to 1 atm=0.101325 MPa values.

<sup>d</sup>Employed a free rotor with  $I^{(2,1)} = 3.0425 \text{ amu } \text{Å}^2$ . The value obtained using the HO approximation for all modes would be  $344.10 \text{ J mol}^{-1} \text{K}^{-1}$ .

<sup>e</sup>Employed free rotors with  $I^{(2,1)} = 2.9989 \text{ amu } \text{Å}^2$ . The value obtained using the HO approximation for all modes would be  $301.99 \text{ J mol}^{-1} \text{K}^{-1}$ .

<sup>f</sup>Includes  $R \ln 3$  for entropy of mixing of isomers.

<sup>g</sup>Mean absolute deviations (|Dev|) and maximum deviations (Max dev) are quoted relative to literature values (molecules with no rotors) or E3 values (molecules with rotors).

same theoretical procedures as used in G2 theory, namely MP2/6-31G(*d*) optimized geometries and scaled HF/6-31G(*d*) harmonic vibrational frequencies. They provide entropies accurate to  $0.5 \text{ J mol}^{-1} \text{K}^{-1}$  at 298 K. For molecules with one internal rotation, E1 uses the harmonic oscillator approximation for all vibrational modes except for very low frequency torsions which are treated as free rotors. It will usually underestimate the third-law entropies, by up to to  $\sim 1.5 \text{ J mol}^{-1} \text{K}^{-1}$ . The E2 and E3 models replace the harmonic oscillator approximation by use of a single cosine potential (calculated at the MP2/6-311+G(2*df*,*p*)/MP2/6-31G(*d*) level) for single-rotor molecules and this gives entropies accurate to  $1 \text{ J mol}^{-1} \text{K}^{-1}$  at 298 K. For molecules with two internal rotations, E1 should be accurate to  $2 \text{ J mol}^{-1} \text{K}^{-1}$  unless the internal rotation barriers are 2-4  $\text{kJ mol}^{-1}$ , in which case the error might be slightly larger, while E2, which uses an independent-mode approximation, will probably be accurate to significantly better than  $2 \text{ J mol}^{-1} \text{K}^{-1}$ . E3, which takes into account the coupling between rotors, should be accurate to  $1 \text{ J mol}^{-1} \text{K}^{-1}$  unless there are many low-frequency modes present. For systems with two neighbouring internal rotors, E3 represents one of the most accurate means of computing third-law entropies reported to date. The E1 procedure, on the other hand, is sufficiently simple and generally gives sufficient accuracy to be suitable for widespread application.

Our investigation of various statistical thermodynamic models for calculating the entropy of an internal rotation shows that significant improvements on harmonic oscillator and free rotor results can be made using tabulated results for single cosine potentials. The harmonic oscillator approximation usually underestimates the entropy, by  $1-2 \text{ J mol}^{-1} \text{K}^{-1}$  at 298 K for internal rotations having barriers between roughly 4 and  $10 \text{ kJ mol}^{-1}$ , but can cause a substantial positive error when the barrier is less than  $\sim 4 \text{ kJ mol}^{-1}$  at 298 K due to its incorrect high-temperature or low-frequency asymptote, by up to  $+23 \text{ J mol}^{-1} \text{K}^{-1}$  in our worst case (toluene). The free rotor model results in overestimates of entropy which are worst in high barrier situations, by up to  $+6 \text{ J mol}^{-1} \text{K}^{-1}$  per internal rotation in the cases studied here. A judicious combination of the harmonic oscillator and free rotor approximations (as in the E1 model) limits the error to rather less than  $2 \text{ J mol}^{-1} \text{K}^{-1}$  per internal rotation. Results using an idealized simple cosine potential (as in the E2 model) are anticipated to be accurate to better than  $1 \text{ J mol}^{-1} \text{K}^{-1}$  for internal rotations for which this potential is reasonable. For species with two internal rotations, various attempts at independent-mode-approximation models (using different choices for uncoupled potentials and partition functions) failed to significantly improve on the accuracy of results using simple individual cosine potentials. In these cases, a treatment involving rotor-rotor potential coupling (as

in the E3 model) gives the most accurate results, and two-dimensional potentials based on MP2/6-311+G(2df,p) energies are presented for the internal rotations of twelve such species.

## ACKNOWLEDGMENTS

We gratefully acknowledge helpful discussions with Dr. Brian Smith and a generous allocation of time on the Fujitsu VP-2200 supercomputer of the Australian National University Supercomputing Facility.

- <sup>1</sup>D. D. Wagman, W. H. Evans, V. B. Parker, R. H. Schumm, I. Halow, S. M. Bailey, K. L. Churney, and R. L. Nuttall, *J. Chem. Phys. Ref. Data* **11**, Suppl. 2 (1982).
- <sup>2</sup>M. W. Chase, Jr., C. A. Davies, J. R. Downey, Jr., D. J. Frurip, R. A. McDonald, and A. N. Syverud, *J. Chem. Phys. Ref. Data* **14**, Suppl. 1 (1985).
- <sup>3</sup>*Lange's Handbook of Chemistry*, edited by J. A. Dean (McGraw-Hill, New York, 1985).
- <sup>4</sup>S. G. Lias, J. F. Liebman, and R. D. Levin, *J. Phys. Chem. Ref. Data* **13**, 695 (1984).
- <sup>5</sup>S. G. Lias, J. E. Bartmess, J. F. Liebman, J. L. Holmes, R. D. Levin, and W. G. Mallard, *J. Phys. Chem. Ref. Data* **17**, Suppl. 1 (1988).
- <sup>6</sup>N. G. Adams, D. Smith, M. Tichy, G. Javehery, N. D. Twiddy, and E. E. Ferguson, *J. Chem. Phys.* **91**, 4037 (1989).
- <sup>7</sup>M. Mautner and L. W. Sieck, *J. Am. Chem. Soc.* **113**, 4448 (1991).
- <sup>8</sup>J. E. Szulejko and T. B. McMahon, *J. Am. Chem. Soc.* **115**, 7839 (1993).
- <sup>9</sup>J. C. Traeger (unpublished).
- <sup>10</sup>B. J. Smith and L. Radom, *J. Am. Chem. Soc.* **115**, 4885 (1993).
- <sup>11</sup>B. J. Smith and L. Radom, *Chem. Phys. Lett.* **231**, 345 (1994).
- <sup>12</sup>M. Gloukhovtsev, J. Szulejko, T. B. McMahon, J. W. Gauld, A. P. Scott, B. J. Smith, A. Pross, and L. Radom, *J. Phys. Chem.* **98**, 13099 (1995).
- <sup>13</sup>B. J. Smith and L. Radom, *J. Phys. Chem.* **99**, 6468 (1995).
- <sup>14</sup>L. A. Curtiss, K. Raghavachari, G. W. Trucks, and J. A. Pople, *J. Chem. Phys.* **94**, 7221 (1991).
- <sup>15</sup>W. J. Hehre, L. Radom, P. v. R. Schleyer, and J. A. Pople, *Ab Initio Molecular Orbital Theory* (Wiley, New York, 1986).
- <sup>16</sup>M. J. Frisch, G. W. Trucks, M. Head-Gordon, P. M. W. Gill, M. W. Wong, J. B. Foresman, B. G. Johnson, H. B. Schlegel, M. A. Robb, E. S. Replogle, R. Gomperts, J. L. Andres, K. Raghavachari, J. S. Binkley, C. Gonzalez, R. L. Martin, D. J. Fox, D. J. DeFrees, J. Baker, J. J. P. Stewart, and J. A. Pople, GAUSSIAN 92 (Gaussian, Inc., Pittsburgh, 1992).
- <sup>17</sup>M. J. Frisch, G. W. Trucks, H. B. Schlegel, P. M. W. Gill, B. G. Johnson, M. A. Robb, J. R. Cheeseman, T. A. Keith, G. A. Petersson, J. A. Montgomery, K. Raghavachari, M. A. Al-Laham, V. G. Zakrzewski, J. V. Ortiz, J. B. Foresman, J. Cioslowski, B. B. Stefanov, A. Nanayakkara, M. Challacombe, C. Y. Peng, P. Y. Ayala, W. Chen, M. W. Wong, J. L. Andres, E. S. Replogle, R. Gomperts, R. L. Martin, D. J. Fox, J. S. Binkley, D. J. DeFrees, J. Baker, J. P. Stewart, M. Head-Gordon, C. Gonzalez, and J. A. Pople, GAUSSIAN 94 (Gaussian, Inc., Pittsburgh, 1995).
- <sup>18</sup>H.-J. Werner and P. J. Knowles, MOLPRO, December 1992 and April 1994 versions (University of Sussex, Sussex, 1992 and 1994).
- <sup>19</sup>P. C. Hariharan and J. A. Pople, *Theor. Chim. Acta.* **28**, 213 (1973).
- <sup>20</sup>R. Krishnan, J. S. Binkley, R. Seeger, and J. A. Pople, *J. Chem. Phys.* **72**, 650 (1980).
- <sup>21</sup>T. Clark, J. Chandrasekhar, G. W. Spitznagel, and P. v. R. Schleyer, *J. Comput. Chem.* **4**, 294 (1983).
- <sup>22</sup>M. J. Frisch, J. A. Pople, and J. S. Binkley, *J. Chem. Phys.* **80**, 3265 (1984).
- <sup>23</sup>T. H. Dunning Jr., *J. Chem. Phys.* **90**, 1007 (1989).
- <sup>24</sup>R. A. Kendall, T. H. Dunning, Jr., and R. J. Harrison, *J. Chem. Phys.* **96**, 6796 (1992).
- <sup>25</sup>C. Møller and M. S. Plesset, *Phys. Rev.* **46**, 618 (1934).
- <sup>26</sup>J. A. Pople, J. S. Binkley, and R. Seeger, *Int. J. Quantum Chem. Symp.* **10**, 1 (1976).
- <sup>27</sup>R. Krishnan and J. A. Pople, *Int. J. Quantum Chem.* **14**, 91 (1978).
- <sup>28</sup>R. Krishnan, M. J. Frisch, and J. A. Pople, *J. Chem. Phys.* **72**, 4244 (1980).
- <sup>29</sup>R. J. Bartlett, *J. Phys. Chem.* **93**, 1697 (1989).
- <sup>30</sup>C. Hampel, K. Peterson, and H.-J. Werner, *Chem. Phys. Lett.* **190**, 1 (1992).
- <sup>31</sup>J. A. Pople, M. Head-Gordon, and K. Raghavachari, *J. Chem. Phys.* **87**, 5968 (1987).
- <sup>32</sup>K. Raghavachari, G. W. Trucks, J. A. Pople, and M. Head-Gordon, *Chem. Phys. Lett.* **157**, 479 (1989).
- <sup>33</sup>M. J. O. Deegan and P. J. Knowles, *Chem. Phys. Lett.* **227**, 321 (1994).
- <sup>34</sup>H. B. Schlegel, *J. Comput. Chem.* **3**, 214 (1982).
- <sup>35</sup>J. F. Gaw and N. C. Handy, *Annu. Rep. R. Soc. Chem. C* **81**, 291 (1984).
- <sup>36</sup>*Geometrical Derivatives of Energy Surfaces and Molecular Properties*, edited by P. Jørgensen and J. Simons (Reidel, Dordrecht, 1986).
- <sup>37</sup>P. Pulay, *Mol. Phys.* **17**, 197 (1969).
- <sup>38</sup>P. Pulay, in *Modern Theoretical Chemistry*, edited by H. F. Schaefer III (Plenum, New York, 1977), p. 153.
- <sup>39</sup>J. A. Pople, R. Krishnan, H. B. Schlegel, and J. S. Binkley, *Int. J. Quantum Chem. Symp.* **13**, 325 (1979).
- <sup>40</sup>N. C. Handy and H. F. Schaefer III, *J. Chem. Phys.* **81**, 5031 (1984).
- <sup>41</sup>M. J. Frisch, M. Head-Gordon, and J. A. Pople, *Chem. Phys. Lett.* **166**, 275 (1990).
- <sup>42</sup>M. J. Frisch, M. Head-Gordon, and J. A. Pople, *Chem. Phys. Lett.* **166**, 281 (1990).
- <sup>43</sup>J. Baker, *J. Comp. Chem.* **7**, 385 (1986).
- <sup>44</sup>H. B. Schlegel, J. S. Binkley, and J. A. Pople, *J. Chem. Phys.* **80**, 1976 (1984).
- <sup>45</sup>K. S. Pitzer and W. D. Gwinn, *J. Chem. Phys.* **10**, 428 (1942).
- <sup>46</sup>K. S. Pitzer, *J. Chem. Phys.* **14**, 239 (1946).
- <sup>47</sup>J. E. Kilpatrick and K. S. Pitzer, *J. Chem. Phys.* **17**, 1064 (1949).
- <sup>48</sup>M. D. Harmony, V. W. Laurie, R. L. Kuczkowski, R. H. Schwendeman, D. A. Ramsay, F. J. Lovas, W. J. Lafferty, and A. G. Maki, *J. Chem. Phys. Ref. Data* **8**, 619 (1979).
- <sup>49</sup>T. Shimanouchi, *Tables of Molecular Vibrational Frequencies I* (National Bureau of Standards, Washington, D.C., 1972).
- <sup>50</sup>A. R. Hoy, I. M. Mills, and G. Strey, *Mol. Phys.* **24**, 1265 (1972).
- <sup>51</sup>J. A. Pople, A. P. Scott, M. W. Wong, and L. Radom, *Isr. J. Chem.* **33**, 345 (1993).
- <sup>52</sup>A. P. Scott and L. Radom, *J. Phys. Chem.* (in press).
- <sup>53</sup>J. C. M. Li and K. S. Pitzer, *J. Phys. Chem.* **60**, 466 (1956).
- <sup>54</sup>S. Bell, *J. Mol. Struct.* **320**, 125 (1994).
- <sup>55</sup>J. A. Pople, M. Head-Gordon, D. J. Fox, K. Raghavachari, and L. A. Curtiss, *J. Chem. Phys.* **90**, 5622 (1989).
- <sup>56</sup>A. Chung-Phillips and K. A. Jøbbert, *J. Chem. Phys.* **102**, 7080 (1995).
- <sup>57</sup>S. Sieber, P. Buzek, P. v. R. Schleyer, W. Koch, and J. W. d. M. Carneiro, *J. Am. Chem. Soc.* **115**, 259 (1993).
- <sup>58</sup>J. Chao, K. R. Hall, K. N. Marsh, and R. C. Wilhoit, *J. Chem. Phys. Ref. Data* **15**, 1369 (1986).
- <sup>59</sup>K. Takagi and T. Kojima, *J. Phys. Soc. Jpn.* **30**, 1145 (1971).
- <sup>60</sup>K. V. L. N. Sastry, E. Herbst, R. A. Booker, and F. C. De Lucia, *J. Mol. Spectrosc.* **116**, 120 (1986).
- <sup>61</sup>W. G. Fateley and F. A. Miller, *Spectrochim. Acta* **17**, 857 (1961).
- <sup>62</sup>G. Włodarczyk, J. Demaison, N. Heineking, and A. G. Császár, *J. Mol. Spectrosc.* **167**, 239 (1994).
- <sup>63</sup>W. G. Fateley and F. A. Miller, *Spectrochim. Acta* **18**, 977 (1962).
- <sup>64</sup>T. Kundu, S. N. Thakur, and L. Goodman, *J. Chem. Phys.* **97**, 5410 (1992).
- <sup>65</sup>P. Groner, G. A. Guirgis, and J. R. Durig, *J. Chem. Phys.* **86**, 565 (1986).
- <sup>66</sup>J. D. Swalen and C. C. Costain, *J. Chem. Phys.* **31**, 1562 (1959).
- <sup>67</sup>R. Peter and H. Dreizler, *Z. Naturforsch. Teil A* **20**, 301 (1965).
- <sup>68</sup>R. Nelson and L. Pierce, *J. Mol. Spectrosc.* **18**, 344 (1965).
- <sup>69</sup>J. M. Vacherand, B. P. van Eijck, J. Burie, and J. Demaison, *J. Mol. Spectrosc.* **118**, 355 (1986).
- <sup>70</sup>D. Cremer, J. S. Binkley, J. A. Pople, and W. J. Hehre, *J. Am. Chem. Soc.* **96**, 6900 (1974).
- <sup>71</sup>P. Bowers and L. Schäfer, *J. Mol. Struct.* **69**, 233 (1980).
- <sup>72</sup>A. Toro Labbe and J. Maruani, *Int. J. Quantum Chem.* **22**, 115 (1982).
- <sup>73</sup>Y. G. Smeyers and A. Huertas-Cabrera, *Theor. Chim. Acta* **64**, 97 (1983).
- <sup>74</sup>L. Radom, J. Baker, P. M. W. Gill, R. H. Nobes, and N. V. Riggs, *J. Mol. Struct.* **126**, 271 (1985).
- <sup>75</sup>Y. G. Smeyers, M. L. Senent, V. Botella, and D. C. Moule, *J. Chem. Phys.* **98**, 2754 (1993).
- <sup>76</sup>H. H. Nielsen, *Phys. Rev.* **40**, 445 (1932).

- <sup>77</sup>J. E. Mayer, S. Brunauer, and M. G. Mayer, *J. Am. Chem. Soc.* **55**, 37 (1933).
- <sup>78</sup>E. Teller and K. Weigert, *Nachr. Ges. Wiss. Göttingen, Math. Phys. Klasse* **218** (1933).
- <sup>79</sup>L. S. Kassel, *J. Chem. Phys.* **3**, 115 (1935).
- <sup>80</sup>L. S. Kassel, *J. Chem. Phys.* **3**, 326 (1935).
- <sup>81</sup>L. S. Kassel, *J. Chem. Phys.* **4**, 276 (1936).
- <sup>82</sup>L. S. Kassel, *J. Chem. Phys.* **4**, 435 (1936).
- <sup>83</sup>K. S. Pitzer, *J. Chem. Phys.* **5**, 469 (1937).
- <sup>84</sup>E. B. Wilson, Jr., *J. Chem. Phys.* **6**, 740 (1938).
- <sup>85</sup>E. B. Wilson, Jr., *Chem. Rev.* **27**, 17 (1940).
- <sup>86</sup>J. S. Koehler and D. M. Dennison, *Phys. Rev.* **57**, 1006 (1940).
- <sup>87</sup>D. G. Burkhard and D. M. Dennison, *Phys. Rev.* **84**, 408 (1951).
- <sup>88</sup>E. V. Ivash and D. M. Dennison, *J. Chem. Phys.* **21**, 1804 (1953).
- <sup>89</sup>W. Weltner, Jr. and K. S. Pitzer, *J. Am. Chem. Soc.* **73**, 2606 (1951).
- <sup>90</sup>E. V. Ivash, J. C. M. Li, and K. S. Pitzer, *J. Chem. Phys.* **23**, 1814 (1955).
- <sup>91</sup>D. R. Herschbach, H. S. Johnston, K. S. Pitzer, and R. E. Powell, *J. Chem. Phys.* **25**, 736 (1956).
- <sup>92</sup>D. M. Grant, R. J. Pugmire, R. C. Livingston, K. A. Strong, H. L. McMurry, and R. M. Brugger, *J. Chem. Phys.* **52**, 4424 (1970).
- <sup>93</sup>D. C. Moule, Y. G. Smeyers, M. L. Senent, D. J. Clouthier, J. Karolczak, and R. H. Judge, *J. Chem. Phys.* **95**, 3137 (1991).
- <sup>94</sup>M. L. Senent, D. C. Moule, and Y. G. Smeyers, *J. Chem. Phys.* **102**, 5952 (1995).
- <sup>95</sup>P. Groner and J. R. Durig, *J. Chem. Phys.* **66**, 1856 (1977).
- <sup>96</sup>P. Groner, J. F. Sullivan, and J. R. Durig, in *Vibrational Spectra and Structure*, edited by Durig, J. R. (Elsevier, Amsterdam, 1981), p. 405.
- <sup>97</sup>See AIP document no. PAPS-JCPA-106-6655-12 for 12 further tables, including the points used in the PES fits plus complete versions of Tables V, VII, XI, XIV, and XVI for all our tested molecules at 298.15 K, 500 K, and 600 K where applicable. Order by PAPS number and journal reference from American Institute of Physics, Physics Auxiliary Publication Service, Carolyn Gehlbach, 500 Sunnyside Boulevard, Woodbury, NY 11797-2999. Fax: 516-576-2223, e-mail: paps@aip.org. The price is \$1.50 for each microfiche (98 pages) or \$5.00 for photocopies of up to 30 pages, and \$0.15 for each additional page over 30 pages. Airmail additional. Make checks payable to the American Institute of Physics.
- <sup>98</sup>J. Chao and B. J. Zwolinski, *J. Chem. Phys. Ref. Data* **5**, 319 (1976).
- <sup>99</sup>J. Troe, *J. Chem. Phys.* **66**, 4758 (1977).
- <sup>100</sup>D. G. Truhlar, *J. Comput. Chem.* **12**, 266 (1991).